Acta Pharmaceutica Sinica B 2026;16(6):3315−3342

Chinese Pharmaceutical Association
Institute of Materia Medica, Chinese Academy of Medical Sciences

Acta Pharmaceutica Sinica B

www.elsevier.com/locate/apsb
www.sciencedirect.com

REVIEW

# Targeting frizzled receptors (FZDs) for anti-tumor therapy: From orthosteric to allosteric inhibition

**Jiaqi Liang[a,†], Yiming Pan[a,†], Zhenyu Kong[a], Boyang Wang[a], Jiantang Yang[b,*], Jing Li[a,*]**

[a]*State Key Laboratory of Oral Diseases & National Center for Stomatology & National Clinical Research Center for Oral Diseases & Research Unit of Oral Carcinogenesis and Management & Chinese Academy of Medical Sciences, West China Hospital of Stomatology, Sichuan University, Chengdu 610041, China*
[b]*Key School and Hospital of Stomatology, Zunyi Medical University, Zunyi 563003, China*

Received 29 October 2025; received in revised form 13 February 2026; accepted 22 February 2026

**KEY WORDS**

Frizzled receptor;
WNT signaling pathway;
Negative allosteric modulator;
Orthosteric inhibitors;
Drug development;
Targeted therapy;
Combination therapy;
Cancer

**Abstract** Frizzled receptors (FZDs) have emerged as pivotal regulators in cancer biology, orchestrating key oncogenic processes such as tumor metastasis, therapy resistance, and stemness through canonical WNT/$\beta$-catenin and noncanonical WNT/PCP and WNT/$Ca^{2+}$ signaling pathways. Their overexpression in diverse malignancies and cell surface localization make FZDs compelling therapeutic targets. Yet, clinical translation of FZD-targeted therapies has been hindered by limited efficacy and poor subtype specificity of FZD orthosteric inhibitors. In this review, we provide a comprehensive and systematic analysis of FZD biology by tracing its discovery history, elucidating its conserved structural features, and deciphering its context-dependent roles in WNT signaling. We propose novel insights into the multifaceted roles of FZD in tumorigenesis, positioning it as a driver of cancer progression. We emphasize the urgent need for developing subtype-selective targeting strategies for FZD, critically assess the challenges of achieving binding specificity within highly homologous extracellular domains, and summarize cutting-edge advances in structure-based design of FZD negative allosteric modulators. This study establishes a strategic framework for precision targeting of the FZD family, paving the way for developing more efficient, mechanism-driven, and potentially transformative anticancer therapies.

*Corresponding authors.
E-mail addresses: xiaoyang198509@163.com (Jiantang Yang), lijing1984@scu.edu.cn (Jing Li).
†These authors made equal contributions to this work.

Peer review under the responsibility of Chinese Pharmaceutical Association and Institute of Materia Medica, Chinese Academy of Medical Sciences.

https://doi.org/10.1016/j.apsb.2026.03.046

## 1. Introduction

The WNT signaling pathway serves as a central signaling hub regulating stem cell self-renewal and tissue homeostasis. Its precise regulation is indispensable for embryonic development. In adult tissues, maintaining this pathway in a quiescent state is crucial for preventing excessive proliferation[1]. However, under pathological conditions, constitutive activation of the WNT pathway plays a core role in the initiation and progression of various solid tumors. Genetic mutations or epigenetic alterations frequently occur in the components of the WNT pathway, leading to oncogene transcription[2]. Currently, conventional therapies have limited efficacy against WNT-dependent tumors and are prone to inducing drug resistance. Approaches directly targeting the core components of this pathway have emerged as a novel strategy[3].

Traditionally, WNT signal transduction was found to be associated with $\beta$-catenin. With the discovery of additional non-$\beta$-catenin signaling components, WNT signaling has now been expanded into multiple branches, including the canonical WNT pathway (WNT/$\beta$-catenin) and noncanonical pathways (WNT/PCP and WNT/$Ca^{2+}$). Among these, the activation of various WNT signaling pathways all requires the involvement of Frizzled (FZD), a seven-transmembrane receptor located on the cell membrane[4,5]. The human FZD family consists of FZD1-10, belonging to Class F G protein-coupled receptors (GPCRs). The extracellular region of FZD contains a cysteine-rich domain (CRD), which is crucial for recognizing and binding WNT ligands. With advances in structural biology, the active sites of the CRD during ligand binding have been elucidated. This has not only deepened the understanding of the aberrant activation mechanism of FZD in cancer, but also provides a structural foundation for CRD-based drug design[6,7]. Currently, orthosteric inhibition is the most common strategy for targeting FZD. It refers to a mechanism that blocks the signaling pathway by binding to the active site of CRD. Drugs that exert orthosteric inhibition are termed orthosteric inhibitors, and their binding sites are referred to as orthosteric binding sites[8]. In 2012, Gurney et al.[9] first demonstrated that the orthosteric inhibitor OMP-18R5 exhibits pan-FZD targeting, capable of blocking multiple WNT signals. However, OMP-18R5 exhibited off-target drug toxicity in clinical trials. As of 2017, all clinical trials related to OMP-18R5 have been terminated. This is primarily because the WNT pathway plays a critical role in maintaining homeostasis in adult tissues, and systemic complete inhibition could trigger severe drug toxicity[10]. The highly conserved character of CRD poses a major challenge in developing highly specific orthosteric inhibitors. Ge et al.[11] proposed achieving precise targeting of FZD subtypes by identifying differentiated CRD binding sites. However, this approach remains challenging and may reduce the binding affinity of orthosteric inhibitors. Therefore, current FZD-targeting strategies have shifted from direct competition at highly conserved orthosteric binding sites toward exploring more selective and druggable binding pockets.

Allosteric effects were initially studied in soluble proteins. Its core lies in the energetic coupling between two structural sites of dynamic proteins[12]. Now, this mechanism has been extended to the activation of proteins. As a dynamically regulated protein, the structural plasticity of FZD allows it to form an activated state by altering the conformation of its transmembrane domain (TMD). Simultaneously, the interaction between FZD and signal transduction proteins influences ligand binding through conformational propagation[13]. This activation mechanism presents an ideal target for allosteric inhibition. Allosteric inhibition can reduce the affinity or efficacy of endogenous ligands by modulating conformation. Drugs that exert allosteric inhibition are termed allosteric negative modulators (NAMs), and their binding sites are referred to as allosteric binding sites[14]. Compared to orthosteric inhibitors, NAMs hold promise for addressing current challenges in targeting FZD due to their high selectivity, favorable safety profile, and ability to incompletely block signaling pathways[15]. However, research on FZD NAMs is still in its infancy and warrants further exploration.

In this review, we first summarize the influence of FZD on different WNT signaling pathways. Then we focus on the multifaceted roles of FZD in cancer progression. Subsequently, we discuss the current status of FZD orthosteric inhibitors in cancer therapy. Finally, we emphasize the necessity and potential of developing NAMs for FZD, offering insights for designing novel FZD-targeted therapeutics in the future.

## 2. The history of FZD

The development of FZDs can be divided into three phases: discovery of the FZDs, exploration of the FZDs structure and biological function, and the FZDs as potential targets for cancer therapy (Fig. 1). The FZD gene was first identified in Drosophila melanogaster in 1982 as a key gene that regulates tissue polarity during development[16]. Vinson et al.[17] found that the protein encoded by this gene possesses a 7-TM structure, featuring both extracellular and cytoplasmic domains, and acts as a key regulator in polarity signaling. Moreover, an extracellular structural domain rich in cysteines was identified *via* FZD gene sequence analysis[18]. The characteristics of this receptor, similar to those of membrane receptors coupled to G proteins, have triggered the exploration of its mechanism of action. Subsequently, Krasnow et al.[19] discovered that FZD and Dishevelled (DVL) form a receptor complex in Drosophila, and proposed that DVL transduces planar polarity signals into the cell to fulfill its function.

In 1996, FZD was identified as receptors for WNT proteins, thereby implicating them in WNT signaling. Studies focusing on the CRD have demonstrated its importance in ligand-receptor interactions[20], which led to the determination of the ligand-free crystal structure of the CRD by 2001[21]. To enhance our understanding of the process of WNT binding to FZD, researchers have resolved the crystal structure of Xenopus WNT8 (XWNT8) in complex with mouse FZD8 (mFZD8) CRD. This revealed a universal binding pattern where WNT envelops the spherical structure of CRD, akin to a hand with thumb and finger[22], engaging at two specific contact sites known as site 1 and site 2. In 2018, the FZD4 TMD was characterized, and researchers have discovered more details of the FZD4 activation mechanism[23]. To further investigate

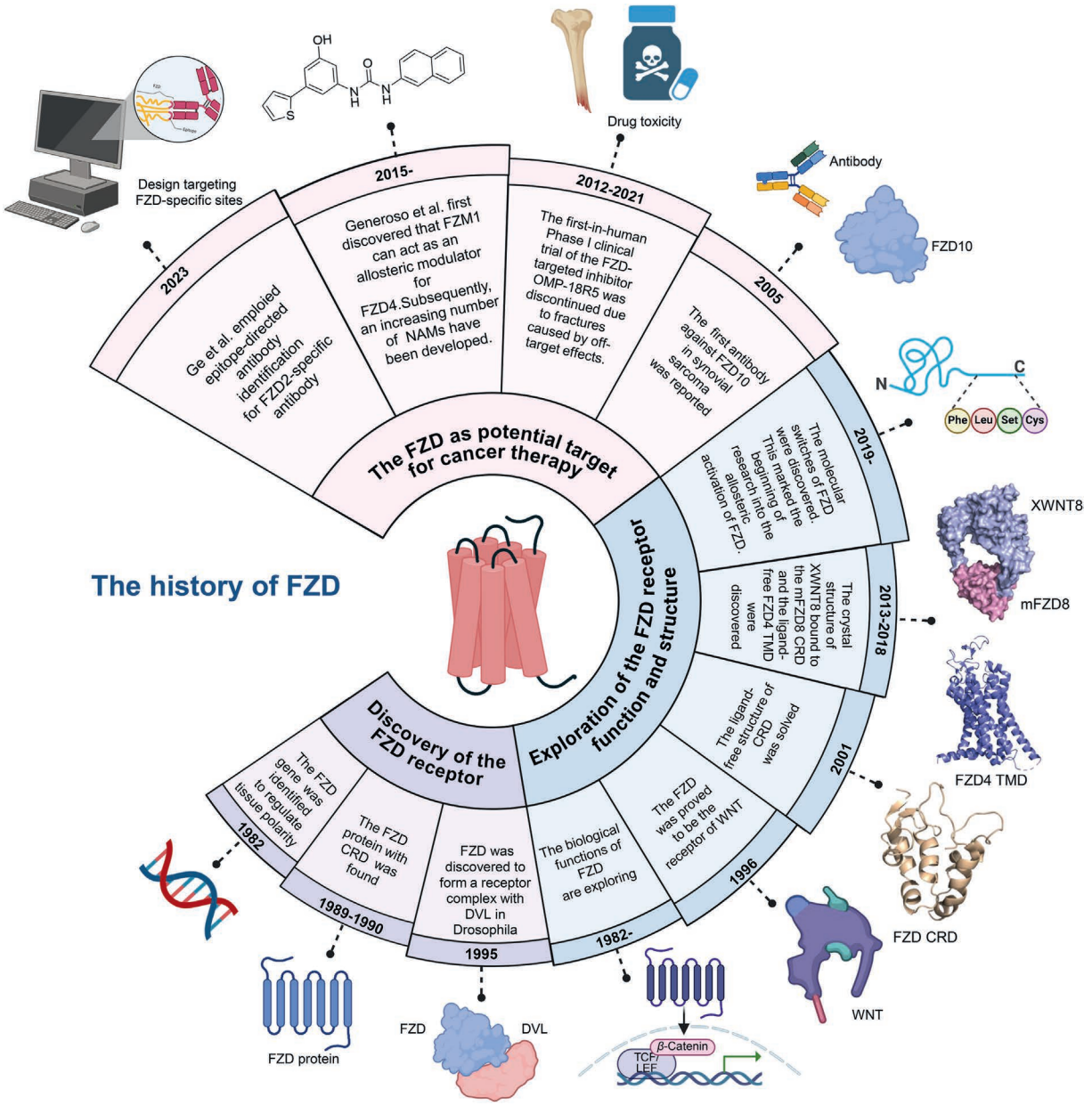


**Figure 1** The history of FZD. From 1982 to 1995, the focus was on exploring the basic biological characteristics of FZD genes and protein molecules. From 1982 to the present, research has expanded to include the functions and mechanisms of action of FZD-encoded proteins. From 2005 to the present, the emphasis has shifted to the exploration of targeted FZD treatments for tumors. FZD, frizzled receptor; CRD, cysteine-rich domain; TMD, transmembrane domain; XWNT8, Xenopus WNT8; mFZD8, mouse FZD8; DVL, Dishevelled.

the activation mechanism of FZD, in 2019, Wright et al.[24] utilized structural analysis and molecular dynamics simulations to identify molecular switches within TM7 that regulate the transition between the active and resting states of FZD. Building on this, Turku et al.[25] further discovered that these molecular switches exist within a broader aromatic network. This marked the beginning of research into the allosteric activation of FZD.

As the mechanisms of the WNT pathway are further elucidated, the important role of FZD in carcinogenesis is becoming clearer. In 1998, research first demonstrated the upregulation of FZD in undifferentiated malignant tissues[26]. As more studies have been conducted, dysregulation of FZD has been shown to contribute to tumorigenesis in numerous cancer types, and FZD has emerged as a promising target for therapy. In 2005, the first reported antibody against FZD10 was tested for its effects on synovial sarcoma (SS)[27]. In 2020, the antibody OMP-18R5 entered Phase I clinical trials as the first reported FZD-antibody[28]. Despite promising anticancer efficacy, challenges such as low subtype specificity and the resulting adverse effects have constrained broader application. The issue of cross-reactivity remains a significant challenge in the development of targeted inhibitors. Ge et al.'s[11] innovative approach employing epitope-directed antibody identification through library and antigen design-assisted studies led to the creation of an FZD2-specific antibody. This represents a promising strategy for optimizing future specific FZD antibodies, potentially overcoming current obstacles in targeted cancer therapy involving FZD. In addition to FZD orthosteric inhibitors, Generoso et al.[29] first

discovered that the pharmacological folding chaperone FZM1 can act as a NAM for FZD4. This provides a rationale for developing novel NAMs for FZDs. Since then, an increasing number of studies have shifted their focus to FZD NAMs. As of 2026, several FZD NAMs have been reported to date[30-35]. Overall, FZD NAMs research has become a key focus for the future development of FZD inhibitors.

## 3. The mechanism of FZD in cancer

As the core receptor of the WNT signaling pathway, FZD exerts multifaceted regulatory functions in cancer initiation and progression by modulating both classical and non-classical signaling pathways. This section first outlines the three major FZD-mediated signaling pathways and the roles of the FZD family in various malignant tumors.

### *3.1. The signaling pathways affected by FZD*

The binding of WNT to specific FZD and their coreceptor initiates intracellular WNT signal transduction, which in turn mediates a variety of physiological functions. However, these signaling pathways can also form a complex regulatory network to play a crucial role in cancer progression. Investigation of WNT signaling elucidates how its aberrant activation contributes to tumor initiation and progression, revealing underlying mechanisms of oncogenesis[36,37].

#### *3.1.1. WNT/β-catenin signaling pathway*

The canonical WNT signaling pathway is mainly composed of WNT ligands, the cell surface receptor complex (FZD and the co-receptors LRP5/6), the cytoplasmic destruction complex, β-catenin, and nuclear TCF/LEF transcription factors[38]. Among these components, β-catenin is the central effector of this pathway. Its activity determines whether the canonical WNT signaling pathway is in the ON or OFF state.

Specifically, in the OFF state, the AXIN protein acts as a scaffold to interact with APC, GSK-3β, and CK1 to form the cytoplasmic destruction complex. The β-catenin is phosphorylated by CK1 and GSK-3β kinases[39]. Subsequently, the phosphorylation motif of β-catenin is targeted by the E3 ubiquitin ligase complex β-TRCP, which induces ubiquitination and proteasomal degradation of β-catenin[40]. This event results in a lack of β-catenin accumulation within the nucleus[41]. At this point, the nuclear TCF/LEF transcription factors bind with the transcriptional repressor GROUCHO, thereby inhibiting the transcription of a series of downstream target genes[42] (Fig. 2A).

In the ON state, WNT binding to the FZD/LRP heterodimer initiates intracellular signaling events. First, the active FZD recruits DVL[43] the cytoplasmic tail of LRP is phosphorylated by GSK-3β and CK1, which leads to the recruitment of AXIN[44,45]. The signaling complex eventually leads to the destructive complex being disturbed. Without the destructive complex, stabilized β-catenin translocates to the nucleus. β-catenin replaces GROUCHO and forms a complex with TCF/LEF to induce the transcription of target genes[46,47]. The orderly ON−OFF regulation of canonical WNT pathways enables it to play a critical role in cancer and other physiological and pathological processes[48] (Fig. 2B).

#### *3.1.2. WNT/PCP signaling pathway*

The WNT/PCP signaling pathway belongs to the non-canonical WNT signaling pathways[49] (Fig. 2C). Upon WNT ligand binding to the receptor, FZD engages several co-receptors, such as receptor tyrosine kinase-like orphan receptor 1/2 (ROR1/2), receptor tyrosine kinase (RYK), and protein tyrosine kinase 7 (PTK7)[50]. Ligand−receptor binding induces the phosphorylation of DVL proteins. Subsequently, DVL-associated activator of morphogenesis (DAAM) and RAC1 are activated. The overall activation process primarily involves two downstream branches[51]. On the one hand, DAAM activates Ras homolog family member A (RHOA). Activated RHOA further induces the activation of Rho-associated coiled-coil containing protein kinase (ROCK) and Diaphanous 1 (DIA1). DIA1 then activates myosin II regulatory light chain (MRLC). On the other hand, RAC1 activates JNK1. JNK1 phosphorylates the c-JUN and CAPZIP proteins. Phosphorylated c-JUN translocates into the nucleus, driving the transcription of downstream target genes. CAPZIP, together with DIA1 and MRLC, participates in promoting actin polymerization[52].

#### *3.1.3. WNT/$Ca^{2+}$ signaling pathway*

Initial identification of the WNT/$Ca^{2+}$ signaling pathway occurred in the 1990s[53]. In the WNT/$Ca^{2+}$ signaling pathway, the co-receptors of FZD include ROR1/2 and RYK[54]. First, the FZD receptor activates the heterotrimeric G protein. The activated G protein then activates phospholipase C (PLC)[5]. Subsequently, PLC catalyzes the production of two important second messengers: inositol 1,4,5-trisphosphate (IP3) and 1,2-diacylglycerol (DAG). IP3 triggers the release of $Ca^{2+}$ from intracellular stores. Consequently, a large amount of $Ca^{2+}$ accumulates in the cytoplasm. Acting as crucial intracellular messengers, these $Ca^{2+}$ activate three classes of downstream effectors: $Ca^{2+}$/calmodulin-dependent protein kinase II (CaMKII), calcineurin (CaN), and protein kinase C (PKC). Furthermore, DAG also participates in activating PKC. The ultimate goal of this activation cascade is to regulate gene transcription. Specifically, CaMKII and CaN act in concert on the transcriptional regulator NFAT, leading to its activation. The activated NFAT translocates into the nucleus and initiates the transcription program of downstream target genes[55] (Fig. 2D).

### *3.2. The multiple roles of FZDs in cancer*

Currently, FZDs have been identified as a crucial regulator in various cancer processes. Different FZD subfamilies exhibit functional biases. For example, FZD1 primarily promotes multidrug resistance in cancer. FZD2 facilitates the epithelial−mesenchymal transition (EMT) process. And FZD4 is mainly associated with tumor angiogenesis. Notably, FZD7 is highly expressed in cancer stem lineages and promotes self-renewal in cancer. FZD10 demonstrates high tumor specificity with minimal expression in normal developmental tissues. These make FZD7 and FZD10 more promising as therapeutic targets[10,56]. Although numerous studies have demonstrated that FZDs play diverse roles in various cancers, a systematic summary remains lacking. Next, we provide a detailed summary of the expression and mechanisms of FZD in different cancers, offering readers a comprehensive understanding of FZD functions (Table 1).

#### *3.2.1. Hepatocellular carcinoma*

Hepatocellular carcinoma (HCC) is the fourth leading cause of cancer-related death, characterized by early-stage concealment, high malignancy, and poor prognosis[122]. During the progression of HCC, FZD plays a critical role. A RT-PCR study showed that abnormal upregulation of FZD occurs in 95% of HCC cells.

Among these FZD subfamilies, the upregulation of FZD3/6/7 is most pronounced, at approximately 30%−40%[123].

Among these FZD subfamilies, FZD7 is the most critical in the progression of HCC[124,125]. FZD7 primarily binds to WNT3, inhibiting the phosphorylation of $\beta$-catenin and promoting its nuclear translocation. This event activates a series of downstream factors and leads to various malignant biological behaviors. For example, the upregulation of FZD7 can activate downstream factors such as c-MYC and cyclin D1, promoting cancer cell proliferation and migration[67,126]. It can also activate the NF-$\kappa$B pathway, contributing to cancer cell survival[127]. Furthermore, the upregulation of FZD7 can promote the expression of cancer stem cell (CSC) markers, as well as drug efflux channels, thereby facilitating the expansion of CSC lineages and the development of drug resistance in cancer[66].

Other FZD subfamilies also demonstrate a high correlation with the malignant biological behavior of HCC. FZD2 is closely associated with the EMT process in HCC. Specifically, the activation of VPS35 can promote the recycling of membrane-localized FZD2, thereby upregulating the activation of downstream WNT/PCP signaling to facilitate EMT[58]. Moreover, FZD2 regulates the EMT process through the FYN/STAT-3/AXL/NUAK1/2 axis. Specifically, the phosphorylation of the Tyr552 site on FZD2 mediates its binding to the SH2 domain of the non-receptor tyrosine kinase FYN, leading to the activation of STAT3. This event activates the receptor tyrosine kinase AXL, which subsequently activates the downstream factors NUAK1/2 to promote the EMT process[59,60]. FZD10 functions mainly through the canonical WNT pathway to mediate HCC biological behaviors, and demonstrates extensive interactions with other pathways. FZD10 activates YAP1 by upregulating canonical WNT signaling, thereby upregulating the HIPPO pathway, which is associated with poor prognosis in HCC. Additionally, FZD10-mediated canonical WNT signaling can activate the c-JUN/MEK/ERK axis, promoting HCC resistance to lenvatinib[71]. The NOTCH1 activation can upregulate canonical WNT signaling *via* FZD10, thereby promoting cell proliferation and survival in HCC[72]. Overall, in HCC, there is significant functional redundancy among FZD subfamilies. This may lead to limited efficacy when targeting a single FZD. Therefore, developing drugs capable of targeting multiple FZD subtypes is a strategy to achieve better therapeutic outcomes in the future.

#### *3.2.2. Lung cancer*

Lung cancer (LC) is the world's leading cancer, with the highest incidence rate among all cancer types. Dysregulation of WNT signaling is a common mechanism driving the development and progression of LC. FZD, as key components of the WNT signaling axis, are frequently upregulated in LC tissues[128]. Current studies have shown that FZD1/3/4/5/7/8/9/10 are abnormally upregulated in LC tissues[73,75,129].

The FZDs primarily regulate the biological behavior of LC cells by mediating the canonical WNT pathway. For example, the activation of the canonical WNT pathway by FZD1 can enhance the chemoresistance of LC cells to cisplatin. Overexpression of miR-135b can reverse chemoresistance by inhibiting FZD1[73]. Another example is that YTHDF1 can enhance the translation efficiency of FZD5 and WNT7B mRNA through m6A modification. The upregulated WNT7B and FZD5 activate the canonical WNT pathway, contributing to various biological processes in LC cells, such as proliferation, migration, and invasion[77]. Additionally, the FZD4 receptor possesses two critical *N*-glycosylation sites: N59 and N144. The absence of *N*-glycosylation causes FZD4 to be retained in the endoplasmic reticulum, ultimately resulting in a complete loss of its ability to activate the Wnt/$\beta$-catenin signaling pathway. In the non-small cell lung cancer (NSCLC) A549 cell model, FZD4 with mutated glycosylation sites fails to promote cancer cell proliferation and migration[76]. In addition to functioning through the canonical WNT pathway, a recent study indicates that FZD3 can also exert oncogenic effects by activating the non-canonical WNT pathway. Specifically, FZD3 interacts with DVL3 to activate the downstream RAC1/JNK pathway. This promotes colony formation, invasiveness, proliferation, and migration abilities of LC cells[75].

It is noteworthy that FZD may exert heterogeneous roles in lung precancerous lesions and cancer. Multiple studies have shown that cigarette smoke can lead to downregulation of FZD9 expression in LC, and promote the malignant transformation of precancerous lesions[130,131]. Meanwhile, other research indicates that WNT can bind to FZD9, activate G$\alpha$16, thereby initiating non-canonical WNT signaling and promoting the proliferation of LC cells[132]. This phenomenon suggests that future studies should focus on the molecular heterogeneity between precancerous lesions and established cancer to prevent potential malignant transformation of precancerous lesions induced by targeted therapeutic strategies.

#### *3.2.3. Gastric cancer*

Statistics show that there are nearly 1 million new cases of gastric cancer (GC) diagnosed worldwide each year, with the highest incidence observed in East Asia[133]. The dysregulation of WNT signaling is closely associated with the progression of GC. As upstream receptors of the WNT pathway, FZD subfamilies are frequently upregulated in GC. A PCR study revealed that FZD1/2/5/7/8 are upregulated in GC tissues[134].

Among these FZD subfamilies, FZD7 plays a critical role in cancer[135]. It primarily promotes cancer cell metastasis, invasion, stemness maintenance, and EMT progression by mediating the canonical WNT signaling pathway[88,136]. Additionally, FZD7 can regulate immune evasion in GC cells by activating non-canonical signaling pathways. Specifically, FPR3 activation upregulates FZD7, which subsequently activates the non-canonical WNT pathway to modulate macrophage polarization. This leads to the formation of an immunosuppressed FPR3+ macrophage lineage, thereby contributing to the remodeling of the immune microenvironment and angiogenesis[137]. Besides FZD7, FZD2/8 also play roles in the progression of GC by canonical WNT signaling transduction, inducing self-renewal and metastasis of GC cells[89,138].

Noteworthy, although FZD5 is upregulated in GC tissues, it has been shown to exert an inhibitory role in the progression of GC. Wang et al.[85] demonstrated that FZD5 binds to WNT7B, which activates the PKC/ELF3 pathway. Specifically, this activation leads to the inhibition of the EMT transcription factor ZEB1, thereby suppressing the EMT process in gastric cancer. This suggests that FZD5 may serve as a GC suppressor and could be used to predict the prognosis of cancer patients[139]. Therefore, therapeutic strategies targeting FZDs necessitate consideration of tissue heterogeneity to enhance precision and thereby mitigate potential risks.

#### *3.2.4. Glioblastoma multiforme*

Glioblastoma multiforme (GBM) is the most common primary intracranial malignant tumor, characterized by its strong invasive capacity and extremely high mortality. Abnormal transduction of the WNT signaling pathway plays a crucial role in the development of GBM. It can promote GBM chemoresistance, regulate

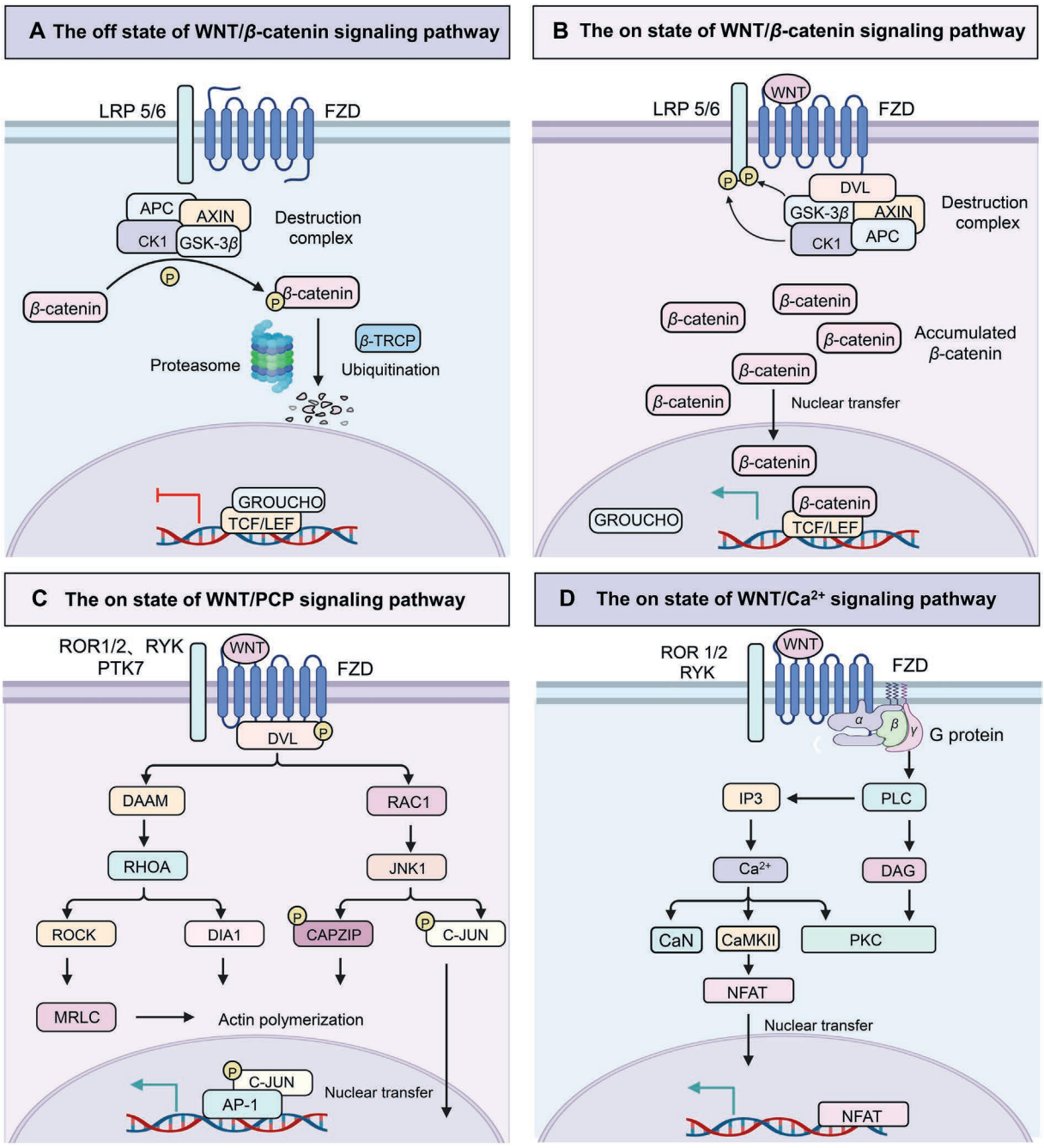


**Figure 2** Overview of the WNT signaling pathways affected by FZD. (A) In the OFF state of the WNT/β-catenin signaling pathway, the destruction complex is formed, which contains GSK-3β, CK1, APC and AXIN. The β-catenin is kept at a low level because of the proteasomal degradation. And TCF/LEF together with GROUCHO suppress the expression of the targeted genes. (B) In the ON state of the WNT/β-catenin signaling pathway, the destruction complex is anchored to the cell membrane. GSK-3β and CK1 phosphorylate LRP5/6. The β-catenin accumulates and transfers into the nucleus to promote the expression of targeted genes. (C) In WNT/PCP signaling pathway, several coreceptors, including ROR1/ROR2, RYK, and PTK7, participate in the activation of this pathway. DVL is activated to bind to DAMM. Subsequently, ROCK, DIA1, MRLC are activated in sequence. Also, DVL can trigger RAC to initiate the JNK signaling cascade. Then c-JUN and CAPZIP are both phosphorylated. In this progress, the actin polymerization is mediated by DIA1, MRLC, and CAPZIP. And the AP-1-dependent gene transcription is promoted by c-JUN. (D) In WNT/$Ca^{2+}$ signaling pathway, coupled heterotrimeric G proteins first activate PLC. Cytoplasmic $Ca^{2+}$ increases *via* the production of IP3 induced by PLC. Subsequently, $Ca^{2+}$-sensitive enzymes such as CaMKII and PKC are activated. In addition, PLC also generates DAG to activate PKC. When NFAT is dephosphorylated by CaMKII and CaN, NFAT enters the nucleus to induce gene transcription. FZD, frizzled receptor; LRP 5/6, low-density lipoprotein receptor-related protein 5/6; APC, adenomatous polyposis coli; AXIN, axis inhibition protein; CK1, casein kinase 1; GSK-3β, glycogen synthase kinase-3β; TCF, T-cell factor; LEF, lymphatic enhancer binding factor; ROR1/2, tyrosine kinase-like orphan receptor 1/2; RYK, tyrosine kinase-related receptor; PTK7, protein tyrosine kinase 7; DAAM, DVL-associated activator of morphogenesis; RHOA, Ras homolog gene-family member A; ROCK, RHO-associated coiled-coil-containing protein kinase;

GBM stemness, and facilitate GBM metastasis and invasion[140]. Studies have shown that FZD2/3/4/5/6/7/9 are upregulated in GBM and actively involved in these functions[92,95,100,141,142]. However, FZD10 is downregulated[101]. The mechanism of action is currently unclear.

In terms of drug resistance formation, FZD5 and FZD6 can mediate GBM resistance to temozolomide. Knockout of FZD6 can sensitize GBM to temozolomide[96]. Moreover, inhibiting FZD5 with ISP-1 suppresses the canonical WNT pathway downstream factors PD-L1 and MGMT. This action sensitizes GBM to temozolomide and counteracts immunosuppression[95].

Regarding GBM stemness and invasiveness, FZD4/7 play major regulatory roles. FZD7 can promote the formation of malignant phenotypes in GBM by mediating both canonical and non-canonical WNT pathways. Liu et al.[98] demonstrated that FZD7 activates the WNT/$\beta$-catenin pathway to enhance GBM stemness acquisition, metastasis, invasion, and the EMT process. Meanwhile, Courtney et al.[99] showed that FZD7 can also bind with VANGL1 to activate downstream RHO GTPases, thereby activating the WNT/PCP pathway and mediating cytoskeletal rearrangement in GBM to promote its metastasis. Given the important role of FZD7 in GBM, multi-cohort validations have identified it as an effective therapeutic target for GBM[143]. FZD4 has also been reported to play a role in GBM stemness and invasiveness. Ahmed et al.[93] indicated that Norrin binding to FZD4 can inhibit the proliferation of ASCL1high GBM stem cells by activating canonical WNT signaling. In contrast, Xun et al.'s[94] research showed that FZD4 promotes mesenchymal phenotype acquisition, stemness and invasiveness in GBM by activating canonical WNT signaling. These contradictory findings suggest that the role of FZD4 in GBM requires further validation and may be closely related to the types of ligands it binds to.

It is worth mentioning that FZD also serves as effective targets for understanding GBM subtypes and their transition mechanisms. In mesenchymal GBM, FZD6 activates the CaMKII/TAK1/NLK pathway while inhibiting canonical WNT signaling. This simultaneously promotes STAT3 and NF-$\kappa$B signaling. Consequently, it drives the acquisition of the mesenchymal phenotype and enhances self-renewal capacity. In neural precursor GBM, FZD6 expression is suppressed, while canonical WNT signaling is activated to promote self-renewal in neural precursor GBM[97]. FZD3 is highly expressed in oligodendrocyte-progenitor-like and neural precursor GBM. By binding to WNT5A, it activates downstream signaling. This activation is associated with a poor prognosis in patients with these subtypes[92]. These findings underscore that GBM is a highly heterogeneous disease, and the role of FZD receptors varies considerably across subtypes. Thus, GBM's dependence on FZD signaling is marked by both subtype-specific and subpopulation-heterogeneous patterns. This intricate landscape complicates the elucidation of core molecular mechanisms and presents a formidable barrier to translating FZD targeting into viable therapies.

#### 3.2.5. *Breast cancer*

Breast cancer (BC) is the most prevalent cancer among women[144]. Abnormal activation of WNT signaling is primarily associated with the initiation of BC[145]. Studies have shown that the upregulation of FZD1/2/3/5/6/7/8/9/10 mediates the abnormal activation of WNT signaling and actively participates in the process of BC initiation[112].

Among these, FZD7 plays the most critical role in regulating BC initiation. First, FZD7 marks the BC initiating cell lineage. FZD7high BC cells exhibit strong tumor forming potential in mouse xenograft models and establish a cellular composition similar to that of the original tumor[146]. Mechanistically, FZD7 activates the canonical WNT signaling pathway, thereby promoting BC cell proliferation and stemness. Additionally, Ping et al.[147] reported that FZD7 activates a non-canonical WNT pathway *via* WNT5A/B binding, modulating a signaling cascade involving p-STAT3, SMAD3, and YAP1 to ultimately drive cell stemness and EMT. Furthermore, FZD1/2/5 have also been reported to activate stemness in BC, potentially contributing to its initiation[102,105,148]. In addition to directly activating BC cell stemness, a recent study has shown that FZD5 can promote BC initiation by regulating the tumor microenvironment. Specifically, the estrogen/cAMP/PKA axis in BC-associated fibroblasts activates FOSL2, which further activates WNT5A. WNT5A binds to FZD5 and activates the NF-$\kappa$B/ERK pathway, thereby promoting angiogenesis and contributing to BC initiation, invasion and metastasis[106].

In addition to tumorigenesis, other BC malignant events also demonstrate a reliance on FZD. For example, FZD5 promotes the nuclear translocation of $\beta$-catenin. This event activates FOXM1, enhancing the expression of BRCA1 and BIRC5 to strengthen the survival ability of BC cells[105]. Furthermore, FZD2 mediates the activation of non-canonical WNT pathways, triggering the NOTCH/TGF-$\beta$ axis to promote the EMT process[103]. The role of FZD in BC pathogenesis is becoming well-established. However, current evidence remains largely confined to triple-negative breast cancer (TNBC). Future research must expand into other BC subtypes to elucidate subtype-specific functions and construct a comprehensive signaling network.

#### 3.2.6. *Osteosarcoma*

Osteosarcoma (OS) is the most common primary bone tumor, characterized by its occurrence in young patients, rapid progression, and strong metastatic potential[149]. As key receptors of WNT signaling, FZD1/3/7/9 are overexpressed in OS[114,116,118-120], exerting both promoting and suppressing regulatory effects in OS. However, FZD6 is downregulated. The mechanism of action is currently unclear[118].

The mechanisms of FZD promoting OS progression have been elucidated. FZD primarily drives OS progression by mediating the activation of downstream factors in the canonical WNT signaling pathway. For example, SNHG10 acts as a molecular sponge for miR-182-5p, upregulating FZD3 expression and enhancing $\beta$-catenin activity, thereby promoting OS progression[116]. Another example is that CircSAMD4A regulates the progression of OS by upregulating FZD7 expression[119]. A limited number of studies have addressed the mechanisms by which FZD inhibits OS progression. FZD suppresses OS progression through activation of canonical WNT signaling. For instance, SPARCL1 activates the WNT/$\beta$-catenin pathway by stabilizing FZD−WNT interactions. This suppresses metastasis and enhances macrophage recruitment

DIA1, diaphanous 1; MRLC, myosin II regulatory light chain; PLC, phospholipase C; IP3, 1,4,5-triphosphate; DAG, 1,2-diacylglycerols; CaMKII, calcium calmodulin-dependent protein kinase II; PKC, protein kinase C; NFAT, nuclear factor associated with T cells; AP-1, activator protein 1; DVL, Dishevelled.

**Table 1** The multiple roles of FZDs in cancer.

| Cancers | FZDs | Expression | Mechanism | Functions | Ref. |
|---|---|---|---|---|---|
| HCC | FZD1 | Upregulated | WNT/β-catenin pathway | Promotion of metastasis, invasion, and proliferation | 57 |
| | FZD2 | Upregulated | WNT/PCP pathway | Promotion of EMT | 58 |
| | | | FYN/STAT-3/AXL/NUAK1/2 axis | Promotion of EMT | 59,60 |
| | FZD3 | Upregulated | WNT/β-catenin pathway | Promotion of proliferation and chemoresistance | 61,62 |
| | FZD4 | Upregulated | NA | Promotion of proliferation, metastasis, and angiogenesis | 63 |
| | FZD5 | Upregulated | WNT/β-catenin pathway | Promotion of stemness and tumorigenesis | 64 |
| | FZD6 | Upregulated | NA | Promotion of proliferation | 65 |
| | FZD7 | Upregulated | WNT/β-catenin pathway | Promotion of stemness, metastasis, proliferation and chemoresistance | 66-68 |
| | FZD8 | Upregulated | WNT/β-catenin pathway | Promotion of metastasis and proliferation | 69 |
| | FZD9 | Upregulated | NA | Promotion of metastasis and proliferation | 70 |
| | FZD10 | Upregulated | WNT/C-JUN/MEK/ERK axis | Promotion of stemness, metastasis, and chemoresistance | 71 |
| | | Upregulated | WNT/β-catenin pathway | Promotion of tumorigenesis | 72 |
| LC | FZD1 | Upregulated | NA | Promotion of chemoresistance | 73 |
| | FZD2 | NA | WNT/β-catenin pathway | Promotion of stemness | 74 |
| | FZD3 | Upregulated | WNT/PCP | Promotion of invasion, proliferation and metastasis | 75 |
| | FZD4 | Upregulated | WNT/β-catenin pathway | Promotion of proliferation and invasion | 76 |
| | FZD5 | Upregulated | WNT/β-catenin pathway | Promotion of invasion, proliferation, and metastasis | 77 |
| | FZD7 | Upregulated | WNT/β-catenin pathway | Promotion of metastasis, and invasion | 78 |
| | FZD8 | Upregulated | WNT/β-catenin pathway | Promotion of invasion, and proliferation | 79 |
| | FZD9 | Upregulated | Noncanonical WNT pathway | Promotion of proliferation | 80 |
| | FZD10 | Upregulated | NA | Promotion of angiogenesis | 81 |
| GC | FZD1 | Upregulated | WNT/β-catenin/SLIT2/ROBO1 | Promotion of fibrosis | 82 |
| | FZD2 | Upregulated | Noncanonical WNT pathway | Promotion of chemoresistance and immune evasion | 83,84 |
| | FZD5 | Upregulated | PKC/ELF3 axis | Inhibition of EMT | 85 |
| | FZD6 | NA | Noncanonical WNT pathway | Promotion of metastasis and proliferation | 86 |
| | FZD7 | Upregulated | WNT/β-catenin/TP63/GPX4 axis | Inhibition of ferroptosis | 87 |
| | | Upregulated | WNT/β-catenin pathway | Promotion of metastasis and invasion | 88 |
| | FZD8 | Upregulated | WNT/β-catenin pathway | Promotion of stemness, chemoresistance, and tumorigenesis | 89 |
| GBM | FZD1 | NA | WNT/β-catenin pathway | Inhibition of autophagy | 90 |
| | FZD2 | Upregulated | NOTCH/NF-κB axis | Promotion of proliferation, angiogenesis, stemness, and EMT | 91 |
| | FZD3 | Upregulated | NA | Poor prognosis | 92 |
| | FZD4 | Downregulated | WNT/β-catenin pathway | Inhibition of stemness | 93 |
| | | Upregulated | WNT/β-catenin pathway | Promotion of stemness and invasion | 94 |
| | FZD5 | Upregulated | WNT/β-catenin pathway | Promotion of chemoresistance | 95 |
| | FZD6 | Upregulated | NA | Promotion of chemoresistance | 96 |
| | | Upregulated | WNT/$Ca^{2+}$/STAT3/NF-κB axis | Promotion of stemness | 97 |
| | FZD7 | Upregulated | WNT/β-catenin pathway | Promotion of stemness, metastasis, invasion, and EMT | 98 |
| | | Upregulated | WNT/PCP pathway | Promotion of invasion, proliferation, and metastasis | 99 |
| | FZD9 | Upregulated | NA | NA | 100 |
| | FZD10 | Downregulated | NA | NA | 101 |
| BC | FZD1 | Upregulated | WNT/β-catenin pathway | Promotion of stemness and chemoresistance | 102 |
| | FZD2 | Upregulated | NOTCH/TGF-β | Promotion of EMT | 103 |
| | FZD3 | Upregulated | WNT/β-catenin pathway | Promotion of invasion, and proliferation | 104 |
| | FZD5 | Upregulated | WNT/β-catenin/FOXM1/BRCA1/BIRC5 axis | Promotion of proliferation, DNA damage repair, and stemness | 105 |
| | | Upregulated | NF-κB/ERK axis | Promotion of angiogenesis, tumorigenesis, and metastasis | 106 |
| | FZD6 | Upregulated | NA | Promotion of invasion, proliferation, and metastasis | 107 |
| | FZD7 | Upregulated | WNT/β-catenin pathway | Promotion of invasion and proliferation, metastasis, stemness, immune evasion, and chemoresistance | 102,108-110 |
| | FZD8 | Upregulated | NA | Promotion of invasion, proliferation, and metastasis | 111 |
| | FZD9 | Upregulated | NA | NA | 112 |
| | FZD10 | Upregulated | WNT/β-catenin pathway | Promotion of metastasis | 113 |
| OS | FZD1 | Upregulated | NA | NA | 114 |
| | FZD2 | NA | WNT/β-catenin pathway | Promotion of stemness | 115 |
| | FZD3 | Upregulated | WNT/β-catenin pathway | Promotion of invasion, proliferation, and metastasis | 116 |
| | FZD4 | NA | WNT/β-catenin pathway | Promotion of invasion and proliferation, metastasis, EMT, and chemoresistance | 117 |
| | FZD6 | Downregulated | NA | NA | 118 |

**Table 1** (*continued*)

| Cancers | FZDs | Expression | Mechanism | Functions | Ref. |
|---|---|---|---|---|---|
| | FZD7 | Upregulated | NA | Promotion of invasion, metastasis, and EMT | 119 |
| | FZD9 | Upregulated | NA | Promotion of invasion, proliferation, and metastasis | 120 |
| | FZDs | NA | WNT/$\beta$-catenin pathway | Inhibition of invasion, metastasis, and immune evasion | 121 |

(1) NA indicates that there is no research reporting the expression, mechanism or functions of this FZD subtype.
(2) AXL, AXL receptor tyrosine kinase; BC, breast cancer; BIRC5, baculoviral IAP repeat containing 5; BRCA1, breast cancer type 1 susceptibility protein; DNMT1/3a, DNA methyltransferase 1/3a; ELF3, E74-Like ETS Transcription Factor 3; EMT, epithelial−mesenchymal transition; ERK, extracellular signal-regulated kinase; FOXF1, forkhead box F1; FOXM1, forkhead box M1; FZD, Frizzled; GC, gastric cancer; GBM, glioblastoma; GPX4, glutathione peroxidase 4; HCC, hepatocellular carcinoma; LC, lung cancer; MEK, MAPK/ERK kinase; NUAK1/2, NUAK family kinase 1/2; OS, Osteosarcoma; PKC, protein kinase C; ROBO1, roundabout guidance receptor 1; SLIT2, slit guidance ligand 2; STAT3, signal transducer and activator of transcription 3; VEGF, vascular endothelial growth factor; YTHDF1, YTH *N*6-methyladenosine RNA binding protein F1.

*via* CCL5 upregulation[121]. In summary, FZDs represent a complex therapeutic vulnerability in OS. Their inhibition carries dual risks. First, it may promote metastasis and immune escape. Additionally, FZDs suppression can redirect osteogenic differentiation to a mesenchymal stem cell fate. This shift may ultimately exacerbate disease progression.

## 4. The structure of FZD

In recent years, advancements in X-ray crystallography, cryo-electron microscopy (cryo-EM), and protein purification techniques have significantly accelerated the structural elucidation of FZD receptors. Currently, numerous studies have reported on the ligand recognition patterns of FZD, the organization of TMD, and the molecular basis of its downstream signal transduction[25]. The available structural information on FZD in different states is directly relevant to the development of FZD inhibitors and their therapeutic efficacy. Therefore, we have systematically reviewed current progress, aiming to provide a structural foundation for subsequent drug development.

FZDs are proteins ranging from 500 to 700 amino acids in length[150]. For drug development, a major obstacle for FZDs is their highly similar amino acid sequences and three-dimensional structures, which poses a challenge for precise therapeutics. Based on sequence similarity, the FZD family is further divided into four subfamilies: FZD1/2/7, FZD3/6, FZD5/8, and FZD4/9/10[151]. Selective targeting among members within a subfamily presents an even greater challenge. To date, only a few FZD orthosteric inhibitors have been reported to specifically target an individual FZD member[29]. Structurally, FZD family members share conserved features, comprising an extracellular region containing the CRD and a linker domain, a 7-TM helix bundle (7 TMD), and an intracellular region[152]. Among them, CRD interacts with WNT and Norrin. The 7 TMD interacts with the DEP domain of DVL and heterotrimeric G proteins. The intracellular region contains a KTXXXW motif that interacts with the PDZ domain of DVL (Fig. 3A).

The CRD is the characteristic domain of FZDs. It forms a globular structure stabilized by disulfide bonds and connects to the receptor core *via* a linker domain[153]. The secreted proteins WNT and Norrin are the primary ligands interacting with the CRD[154]. Notably, Norrin is a specific ligand for the FZD4 CRD and plays key roles in retinal vascular development and maintenance of the blood−retinal barrier[155]. Ke et al.[156] reported that Norrin binds to the FZD4 CRD by forming a dimeric structure. In its free monomeric state, Norrin exhibits a flat, rigid architecture composed of $\beta$-strands and loop regions. Upon approaching the CRD binding interface, Norrin forms a dimeric structure *via* three intermolecular disulfide bonds, including symmetric C93−C95/C95−C93 bonds and a C-terminal C131−C131 bond. Ultimately, the dimeric Norrin engages two CRDs, forming a 2:2 complex with FZD4[156]. At the symmetric binding interface, two $\beta$-hairpin motifs of Norrin approach the CRD[157]. Notably, a hydrophobic core exists within this binding interface, providing the forces for stable interaction with the FZD4 CRD. This hydrophobic core is primarily formed by tight stacking of nonpolar side chains, including V45, M59, L61, L124 from Norrin and F96, M105, I110, M157, M159 from CRD[158] (Fig. 3B). Studies indicate that the FZD4 residues constituting the Norrin binding interface are not conserved in other FZD family members. This implies that other FZD proteins lack a binding pocket correctly shaped to accommodate Norrin, explaining Norrin's extremely high specificity for FZD4[158]. Therefore, targeting the specific residues involved in Norrin-FZD4 recognition holds promise for developing FZD4-selective inhibitors. In 2012, Janda et al.[22] first elucidated the binding mechanism between the CRD and WNT (Fig. 3C). They described the co-crystal structure of XWNT8 with mFZD8 as a two-site handshake model. In this model, the N-terminal $\alpha$-helical domain of XWNT8 forms the palm and thumb. The Palmitic acid (PAM) linked to Ser187 at the tip of the thumb inserts into a hydrophobic groove on the surface of CRD Site I. The C-terminal cysteine-rich domain of XWNT8 forms the index finger. A loop between the Cys315-Cys325 disulfide bond at its tip inserts into a depression at Site II, interacting *via* hydrophobic forces[22]. Currently, the design strategy for FZD orthosteric inhibitors is primarily based on the WNT-CRD binding model.

TMD is a traditional site for many GPCR-targeting drugs[159]. To investigate the structural basis for targeting the FZD TMD, Yang et al.[160] determined the high-resolution crystal structure of the human FZD4 TMD in the ligand-free state (Fig. 3D). The TMD of FZD4 adopts the classic seven-transmembrane helix fold. Its TM6 is shorter and structurally compact, a feature distinct from other known GPCR structures. Compared to the Smoothened (SMO) receptor, FZD4 has a shorter third extracellular loop (ECL3), resulting in a smaller interface between its CRD and TMD, which permits greater CRD mobility. More importantly, the conserved transmembrane pocket of FZD4 contains two extremely narrow bottleneck regions that hinder the access of conventional ligands. This explains why the development of small-molecule ligands targeting FZDs is highly challenging[160].

The TMD and intracellular regions contain multiple sites to communicate with downstream transducer proteins, including DVL and G proteins[161]. In 2016, Gammons et al.[162] demonstrated

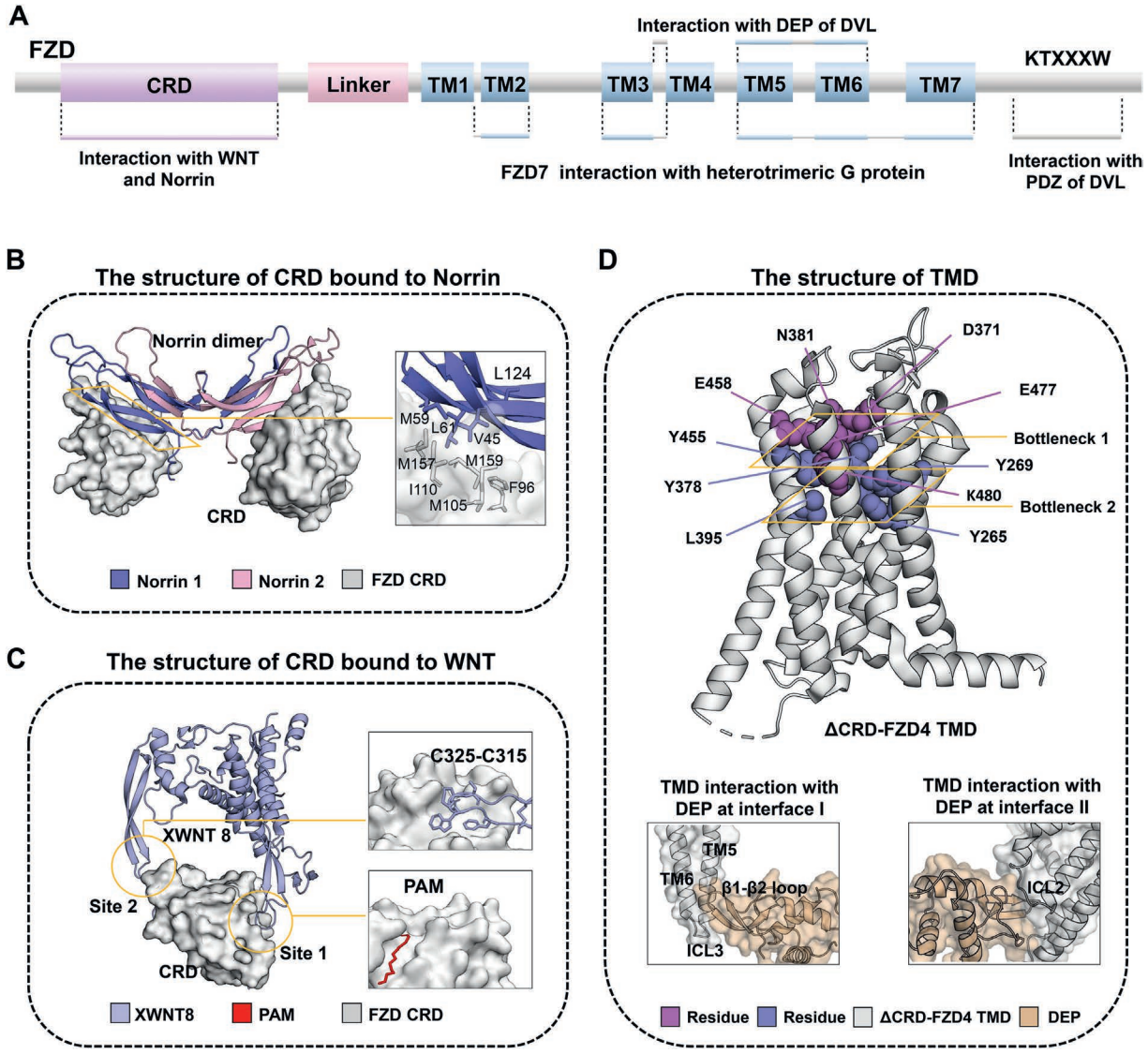


**Figure 3** The structure of FZD. (A) The canonical 7-TM topology of FZD. Extracellularly, the conserved CRD serves as the primary site for WNT and Norrin, which is essential for receptor activation. The linker domain connects the CRD to the transmembrane core and plays a critical role in propagating conformational changes during signal transduction. The 7-TM helix bundle interacts with the DEP domain of DVL and heterotrimeric G proteins. Specifically, TM5, TM6, and the ICL3 between them, together with the DEP domain, constitute the first interface. The ICL2 between TM3 and TM4, along with the DEP domain, forms the second interface. FZD7 communicates with the heterotrimeric G protein through TM2, TM3, TM5, TM6, TM7, as well as ICL1 between TM1 and TM2, and ICL2 between TM3 and TM4. On the intracellular side, the intracellular tail contains the KTxxxW motif that is directly involved in recruiting the PDZ of DVL. (B) The structure of CRD bound to Norrin (PDB:5BQE). Among them, Norrin is shown in pink and blue, and CRD is shown in gray. The right panel illustrates the interface between Norrin and the CRD. (C) The structure of CRD bound to WNT (PDB:4F0A). Among them, WNT is shown in slate, PAM in red, and CRD in gray. The right panel illustrates the interface between Site 1 and Site 2. (D) The structure of TMD. The top panel shows the FZD4 TMD structure without the CRD (PDB:6BD4). The sphere representation highlights two bottlenecks along with key amino acid residues. Below is the interaction interface between TMD and DEP (PDB:8WMA). The residues constituting the bottlenecks of the TMD are colored blue and purple. The TMD is colored gray, and the DEP domain is colored wheat. FZD, frizzled; CRD, cysteine-rich domain; TMD, transmembrane domain; XWNT8, Xenopus WNT8; mFZD8, mouse FZD8; PAM, palmitoleic acid; DVL, dishevelled.

the crucial role of the DEP domain of DVL in activating WNT signaling. To further elucidate the molecular mechanism of the interaction between FZD and the DEP domain, Qian et al.[163] resolved the cryo-EM structure of the FZD4 complex with the DEP domain of DVL2 (Fig. 3D). The study revealed two key interfaces for the FZD4-DVL2 binding. FZD4 forms a hydrophobic interface I *via* TM5, ICL3, and TM6. The DEP domain of DVL inserts its finger-loop structure (the $\beta1-\beta2$ loop) into the hydrophobic pocket of FZD4. Interface II is a polar interface. The ICL2 loop of FZD4 inserts into the groove between the DEP finger loop and the C-loop. Sequence alignment shows that the key residues of interfaces I and II are highly conserved across FZD1-10 and DVL1-3, suggesting that all FZD-DVL interactions may share a common mechanism[163]. To investigate the molecular

mechanism of FZD-G protein communication, Xu et al.[164] resolved the cryo-EM structure of the FZD7 complex with the heterotrimeric G protein $mG_s$. A binding interface distinct from that of the FZD-DVL interaction was identified. The core feature of this interface is the insertion of the far C-terminal segment of the mG$\alpha$s $\alpha$5-helix into the transmembrane helix bundle of FZD7. Within it, the C-terminal leucine residues $L393^{H5.25}$ and $L394^{H5.26}$ form extensive interactions with multiple residues of FZD7, constituting a locally convergent stabilization network[164]. The interactions of DVL and G proteins with FZD exhibit antagonistic roles in cancer development. For instance, in pancreatic cancer, the DVL-mediated WNT/$\beta$-catenin signaling pathway induces the transcriptional activity of GLUT1, promoting tumor growth[165]. In contrast, the G protein-mediated WNT/$Ca^{2+}$ signaling pathway exhibits tumor-suppressive effects[166]. Based on this, developing FZD inhibitors that selectively regulate the DVL and G protein pathways by targeting specific interface sites holds significant clinical importance.

## 5. Current situation of FZD orthosteric inhibitors

FZD orthosteric inhibitors represent the main class of FZD inhibitors and are broadly divided into small molecule inhibitors and protein inhibitors (Table 2). These inhibitors target the FZD CRD to suppress the activation of cancer-associated WNT signaling pathways. Although these agents have demonstrated promising anticancer efficacy in both preclinical studies and clinical trials, toxicity resulting from off-target effects remains a major obstacle.

### 5.1. *Small molecule inhibitors*

Small molecule inhibitors offer distinct advantages, such as high permeability, low risk of immune-related adverse reactions, and good oral bioavailability[178]. However, the number of reported small molecule inhibitors targeting FZD receptors is currently limited. By virtual screening based on the FZD8 CRD and cellular assays, Lee et al.[167] successfully identified small molecule inhibitors with micromolar $IC_{50}$ values (2124-0331, 1094-0205, 3235-0367, NSC36784, NSC654259). In HEK293T cells, all five small molecule inhibitors effectively suppressed the phosphorylation level of Ser1490 on LRP6, indicating their potency in inhibiting the canonical signaling pathway. Among the five inhibitors, NSC36784 and NSC654259 exhibited the strongest activity. However, despite their high potency, the core CRD binding residues such as L97, M149, and D150 are highly conserved across FZD1-FZD10, suggesting these compounds may cross-bind to the CRDs of other FZD subtypes[167]. Given the crucial role of the FZD family in regulating tissue homeostasis, the drug safety profiles of NSC36784 and NSC654259 require further investigation.

Another research team, based on the role of PAM in activating the WNT pathway, screened the ZINC database[168]. By assessing the binding free energy between FZD7 CRD complexes and candidate ligands *via* molecular docking, they identified 30 commercially available ligands with over 99% similarity to PAM. Among them, ZINC05972969 and ZINC04529321 exhibited more favorable binding free energies than PAM (ZINC08221009). The inhibitory mechanism was attributed mainly to ZINC05972969 forming two hydrogen bonds with K61 and Q55, thereby promoting hydrophobic interactions[168]. However, despite the identification of high-affinity small molecule inhibitors for FZD7, future studies are still required to further investigate their anti-tumor effects against FZD7-high tumors.

FZD7 is a key oncogenic driver in GBM. To target FZD7, Sun et al.[143] performed high-throughput virtual screening of 10,000 phytochemicals against the CRD of FZD7. The results indicated that Cycloartobiloxanthone (CAX) was the top inhibitor candidate. Its binding energy with FZD7 was $-8.6$ kcal/mol, and the MMPBSA binding free energy was $-65.2 \pm 3.8$ kcal/mol. Furthermore, CAX possesses excellent pharmacological properties, including high gastrointestinal absorption, low toxicity ($LD_{50} = 2500$ mg/kg), and a blood−brain barrier penetration score of 0.7, which could effectively address the drug delivery challenges in GBM. However, the current findings are based solely on computational simulations. Future studies are required to validate the anti-tumor efficacy of CAX against GBM[143].

### 5.2. *Protein inhibitors*

OMP-18R5 is the first identified pan-FZD monoclonal antibody, targeting FZD1/2/5/7/8[9]. OMP-18R5 primarily binds to a discontinuous epitope on the FZD CRD, located within a cleft region. This region is highly conserved across the FZD family and serves as a critical binding site. In multiple preclinical studies, OMP-18R5 monotherapy or combination therapy with chemotherapy demonstrated promising therapeutic efficacy in various tumors. However, OMP-18R5 does not simply enhance the cytotoxicity of chemotherapy but remodels tumor cell responses to chemotherapy by regulating gene expression. For example, OMP-18R5 combination therapy can suppress paclitaxel-induced expression of stress response genes and ABC transporters, thereby reducing drug resistance. OMP-18R5 combination therapy can block gemcitabine-induced expression of EMT genes[9]. Furthermore, OMP-18R5 can reduce tumor-initiating cell (TIC) frequency, both as monotherapy and in combination therapy[9]. Currently, OMP-18R5 has been evaluated in combination with various chemotherapy regimens in several phase Ib studies, involving treatment of advanced solid tumors (NCT01345201), metastatic pancreatic cancer (NCT02005315), NSCLC (NCT01957007), and BC (NCT01973309).

Given that the FZD receptor targeting spectrum of OMP-18R5 does not include FZD4. But FZD4 is aberrantly overexpressed in various cancers, such as leukemia, GBM[154]. Therefore, expanding the target range of OMP-18R5 is considered to have certain clinical significance. Zvezdan et al.[170] obtained the F2 antibody, which shares an identical binding profile with OMP-18R5, by screening a native Fab library. Subsequently, a second-generation phage library was constructed. In this library, three HCDRs were diversified using a soft randomization strategy, where each codon was designed to encode approximately 50% wild-type sequence and 50% mutations. This process ultimately yielded the variant F2.A. The binding spectrum of F2. A was extended to include FZD4, and it exhibited sub-nanomolar affinity for FZD1/2/4/5/7/8, which is significantly higher than that of F2 and OMP-18R5[170]. In the RNF43-mutant pancreatic ductal adenocarcinoma (PDAC) cell line HPAF-II, F2. A significantly inhibited WNT pathway activation and induced G0/G1 phase arrest and proliferation inhibition. Furthermore, in a fibrin gel microsphere assay coated with human umbilical vein endothelial cells (HUVECs), F2. A significantly inhibited endothelial tube extension, whereas IgG F2 and OMP-18R5 were ineffective[170]. These results indicate that F2. A can inhibit FZD4, thereby exerting anti-angiogenic effects. It is noteworthy that the Norrin-FZD4 signaling pathway is

**Table 2** The FZD orthosteric inhibitors.

| Names | Types | Targets | Status | Effects | Ref. |
|---|---|---|---|---|---|
| 2124-0331 | Small molecule inhibitor | FZD8 CRD | Preclinical | | |
| 1094-0205 | Small molecule inhibitor | FZD8 CRD | Preclinical | | |
| 3235-0367 | Small molecule inhibitor | FZD8 CRD | Preclinical | Inhibition of WNT3A signaling and LRP6 phosphorylation in 3T3 cells. | 167 |
| NSC36784 | Small molecule inhibitor | FZD8 CRD | Preclinical | | |
| NSC654259 | Small molecule inhibitor | FZD8 CRD | Preclinical | | |
| ZINC04529321 | Small molecule inhibitor | FZD7 CRD | Preclinical | Not determined. | 168 |
| ZINC05260769 | Small molecule inhibitor | FZD7 CRD | Preclinical | Not determined. | |
| CAX | Small molecule inhibitor | FZD7 CRD | Preclinical | Not determined. | 143 |
| pF8_AC3 | Protein inhibitor | FZD5/8 CRD | Preclinical | Inhibition of signaling through FZD8 and FZD5 in FZD127-KO 293T and HeLa cells. | 169 |
| sF8_AG6 | Protein inhibitor | FZD8 CRD | Preclinical | Inhibition of signaling through FZD8 in FZD127-KO 293T and HeLa cells. | |
| TT641 pAb | Protein inhibitor | FZD10 CRD | Preclinical | Significant induction of ADCC in SS cells overexpressing FZD10. | 27 |
| F2 | Protein inhibitor | FZD1/2/5/7/8 CRD | Preclinical | Inhibition of the WNT signaling pathway in RNF43 mutant PDAC cell lines. | 170 |
| F2. A | Protein inhibitor | FZD1/2/4/5/7/8 CRD | Preclinical | Induction of G0/G1 phase arrest in HPAF-II cells. | |
| MAb 92-13 | Protein inhibitor | FZD10 CRD | Preclinical | No direct cytotoxicity in SS cells. | 171 |
| $^{90}$Y-MAb 92-13 | Protein inhibitor | FZD10 CRD | Preclinical | Rapid reduction of tumor size in the SYO-1 SS xenograft nude mouse model. | |
| FZD7-NS | Protein inhibitor | FZD7 CRD | Preclinical | Decrease in TNBC cell proliferation. | 172 |
| IgG-2919 | Protein inhibitor | FZD5 CRD | Preclinical | A dose-dependent antiproliferative effect in | 173 |
| IgG-2921 | Protein inhibitor | FZD5 CRD | Preclinical | RNF43-mutant PDAC cell lines. | |
| F2.I | Protein inhibitor | FZD1/2/4/5/7/8 CRD | Preclinical | Highly effective inhibition of WNT signaling, but significant intestinal toxicity *in vivo*. | 174 |
| F7.B | Protein inhibitor | FZD1/2/4/5/7/8 CRD | Preclinical | Good tolerability, but extremely low systemic exposure. | |
| F6 | Protein inhibitor | FZD1/2/5/7/8 CRD | Preclinical | Good tolerability and adequate systemic exposure, but no FZD4 binding. | |
| F2.Iv2 | Protein inhibitor | FZD1/2/4/5/7/8 CRD | Preclinical | Effective inhibition of tumor growth in pancreatic cancer models | |
| scFv-I | Protein inhibitor | FZD7 CRD | Preclinical | | |
| scFv-II | Protein inhibitor | FZD7 CRD | Preclinical | Significant inhibition of TNBC cell proliferation | 175 |
| scFv-III | Protein inhibitor | FZD7 CRD | Preclinical | | |
| F7-ADC | Protein inhibitor | FZD7 CRD | Preclinical | Inhibition of FZD7-high ovarian cancer cells. | 176 |
| OMP-18R5 | Protein inhibitor | FZD1/2/5/7/8 CRD | Clinical trial termination (NCT01345201; NCT02005315; NCT01957007; NCT01973309) | Severe bone toxicity | 9 |
| sF2_C11 | Protein inhibitor | FZD2 CRD | Preclinical | Effective inhibition of the WNT/FZD2 signaling pathway. | 11 |
| sF7_A2 | Protein inhibitor | FZD7 CRD | Preclinical | Priority inhibition of the WNT/FZD7 signaling pathway. | |
| OTSA101 | Protein inhibitor | FZD10 CRD | Clinical trial termination (NCT04176016; NCT01469975) | Hematologic toxicity | 177 |

(1) FZD, Frizzled; CRD, cysteine-rich domain; ADC, antibody–drug conjugates; TNBC, triple-negative breast cancer; scFv, single-chain variable fragments; PDAC, pancreatic ductal adenocarcinoma; SS, synovial sarcoma; CAX cycloartobiloxanthone.

involved in normal physiological processes such as retinal vascular development, and its dysfunction can lead to severe diseases like Norrie disease and familial exudative vitreoretinopathy (FEVR)[179]. F2. A specifically inhibits WNT/FZD4-dependent angiogenic processes without interfering with Norrin-mediated normal physiological signaling, thereby avoiding disruption of vascular homeostasis.

Raman et al.[174] also obtained three pan-FZD monoclonal antibodies (F2.I, F7.B, F6) using phage display technology. Among them, F2.I and F7.B can bind to FZD1/2/4/5/7/8, while F6 has the

same binding profile as OMP-18R5. X-ray crystallography revealed that these antibodies all target the hydrophobic cleft of the CRD to block the binding of WNT ligands to FZD. However, the initial antibodies had significant drawbacks. F2.I caused severe gastrointestinal toxicity due to excessively high affinity for FZD5/7 ($K_d$ = 1.7 and 0.3 nmol/L, respectively)[174]. F7.B exhibited extremely low *in vivo* plasma exposure due to the high hydrophobicity of its CDR regions. F6, lacking FZD4 binding capability, had limited therapeutic coverage. Structure-informed precision engineering provided a solution. By mutating key residues involved in F2.I's binding to FZD5 to moderately reduce its affinity, the variant F2.Iv2 was successfully generated[174]. This variant retained multispecific binding capability for FZD1/2/4/5/7/8, completely alleviated gastrointestinal toxicity, and showed significantly improved plasma exposure. In an RNF43-mutant HPAF-II pancreatic cancer xenograft model, F2.Iv2 achieved a 77% tumor growth inhibition rate, significantly outperforming F6 (56%) and OMP-18R5 (49%)[174]. This study confirmed that structure-guided antibody engineering can address the tolerability and pharmacokinetic challenges of multispecific FZD antibodies by finely tuning properties such as binding affinity and hydrophobicity.

The proliferation of RNF43-mutant PDAC cells is dependent on the WNT/FZD5 signaling pathway[173]. FZD5 antibodies are considered as a potential therapeutic strategy for this tumor type. Steinhart et al.[173] obtained two high-affinity Fabs against FZD5 (Fab-2919, Fab-2921) using phage display technology and converted them into full-length IgG1 antibodies, IgG-2919 and IgG-2921. In RNF43-mutant PDAC cell lines, IgG-2919 and IgG-2921 exhibited dose-dependent anti-proliferative effects. Flow cytometry analysis revealed that antibody treatment induced G0/G1 phase arrest in RNF43-mutant cells without caspase-3 activation[173]. Furthermore, in subcutaneous HPAF-II xenograft models and orthotopic HPAF-II/AsPC-1 pancreatic cancer models, IgG-2919 and IgG-2921 demonstrated a high tumor inhibition rate[173].

SS is a malignant tumor of mesenchymal origin, classified as an adult spindle cell sarcoma, which exhibits resistance to chemotherapy and radiotherapy[180]. Notably, FZD10 is highly expressed in SS cells but shows low or no expression in vital normal organs[27]. Therefore, targeting FZD10 can reduce toxicity to normal tissues. Nagayama et al.[27] developed an FZD10 antibody named TT641 pAb. TT641 pAb can induce antigen-dependent cell-mediated cytotoxicity (ADCC) against SS cells. In a nude mouse xenograft model, intratumoral injection of TT641 pAb for five consecutive days resulted in significantly smaller tumor volumes compared to the group treated with non-immune rabbit IgG[27]. Currently, TT641 pAb remains a polyclonal antibody. Subsequent development of a humanized anti-FZD10 monoclonal antibody is possible for the clinical treatment of SS. Fukukawa et al.[171] successfully developed a mouse-derived monoclonal FZD10 antibody, MAb 92-13. Vivo experiments demonstrated that the monoclonal antibody MAb 92-13 specifically accumulates in SS xenografts and is internalized by tumor cells. Radioimmunotherapy using yttrium-90 ($^{90}$Y)-labeled MAb 92-13 showed that a single intravenous injection significantly inhibited tumor growth, and prolonged time to tumor progression[171]. Similarly, Sudo et al.[177] employed actinium-225 ($^{225}$Ac)-labeled anti-FZD10 antibody OTSA101 and compared it with the same antibody labeled with $^{90}$Y. The results showed that $^{225}$Ac-labeled OTSA101 binds to SYO-1 SS cells *in vitro* comparable to that of indium-111 ($^{111}$In)-labeled anti-FZD10 imaging agent. *In vivo* biodistribution studies demonstrated high tumor and low uptake in normal organs. Dosimetric analysis revealed that the biologically effective dose of $^{225}$Ac-OTSA101 to tumors exceeded that of $^{90}$Y-OTSA101 by 7.8 Bd. In the SYO-1 tumor-bearing mouse model, both labeled antibodies inhibited tumor growth and extended survival[177]. However, only $^{225}$Ac-OTSA101 induced complete remission without recurrence in 60% of the mice for the duration of the study. Furthermore, $^{225}$Ac-OTSA101 induces more tumor necrosis and apoptosis than $^{90}$Y-OTSA101 [177]. The radiation dose to normal tissues was within an acceptable range, with no significant toxicity noted in treated animals. However, in clinical trials, both studies of the radiolabeled monoclonal antibody OTSA101 (NCT04176016; NCT01469975) have been terminated, primarily due to hematologic toxicity caused by the high-energy $\beta$ radiation.

Nanoparticles surface modification on antibody can enhance target affinity and reduce the required dose through multivalent binding effects[172]. Rachel et al.[172] constructed FZD7-nanoshell (NS). The NS possesses good biocompatibility and allows for simple antibody conjugation *via* gold-sulfur bonds. In TNBC cells, treatment with FZD7-NS led to a significant decrease in $\beta$-catenin protein levels. In contrast, free FZD7 antibody at a dose 50 times higher than that of FZD7-NS only showed weak inhibition. The results demonstrate that FZD7 antibody-functionalized NS significantly enhance the inhibitory effect on the WNT signaling pathway in TNBC cells[172].

ADCs are therapeutic agents comprising a monoclonal antibody covalently linked to a cytotoxic drug *via* a linker[176]. Their advantage lies in combining potent antitumor activity with antigen-specific targeting. Myan et al.[176] designed an ADC named F7-ADC by conjugating a human-mouse chimeric IgG1 FZD7 antibody with the microtubule inhibitor monomethyl auristatin E (MMAE). Its conjugation mechanism primarily relies on the cleavable linker of the FZD7 antibody (MC-VC-PABC). Regarding its anticancer mechanism, F7-ADC first recognizes FZD7 on the cell membrane, then internalizes into cytoplasmic lysosomes. Cathepsin B cleaves the MC-VC-PABC linker to release MMAE, which kills the tumor cells[176]. In MA-148 and PA-1 cells with high FZD7 expression, the $IC_{50}$ of F7-ADC was 5 nmol/L. The FZD7 antibody without conjugated MMAE showed no cytotoxicity against any cells, indicating that the toxicity depends on MMAE release and that the F7-Ab itself does not interfere with FZD7's survival-related functions[176]. Furthermore, in xenograft models, F7-ADC can efficiently and selectively kill FZD7-positive ovarian cancer cells.

Single-chain variable fragments (scFvs) offer advantages such as humanization, ease of penetration into tumor tissues, and high affinity[175]. Neda et al.[175] designed scFvs targeting the FZD7 CRD (scFv-I, scFv-II, scFv-III). In antigenic epitope screening, two sites (DAGLEVHQFYPLVKV and PVCTVLDQAIPPCRS) are located near the FZD7 binding epitope and can block WNT/FZD7 interaction through steric hindrance effects. In terms of anticancer activity, all three scFvs can inhibit the proliferation of TNBC cells and induce apoptosis by preventing FZD7 activation[175].

The CRDs of FZD5 and FZD8 share 80% homology. Antibodies targeting FZD8 may potentially inhibit FZD5 signaling pathway activation[169]. Based on this, Li et al.[169] developed an FZD8-specific antibody. First, a first-generation phage library was constructed to screen for FZD8-preferential antibodies. Using the FZD10 antibody hB9L9.3 as a template, random mutations were introduced *via* NNK degenerate codons into the three light chain CDRs and the heavy chain HCDR3 region. During screening, FZD8-CRD served as the positive antigen, while an Fc protein served as the negative antigen to exclude non-specifically binding

antibodies[169]. After four rounds of biopanning, the candidate antibody pF8_AC3 ($EC_{50}$ = 1.70 nmol/L) was selected. pF8_AC3 binds to the Site I region of the FZD8-CRD. Due to the high residue identity in the Site I region, pF8_AC3 still exhibited significant cross-reactivity with FZD5 ($EC_{50}$ = 33.55 nmol/L)[169]. To obtain an FZD8-specific antibody, Lee et al.[169] performed soft randomization mutagenesis on the LCDR3 and HCDR3 of pF8_AC3, which preserved the core hydrophobic residue Y108. During screening, FZD5-CRD was used as a negative antigen to deplete phages. Ultimately, the FZD8-specific antibody sF8_AG6 ($EC_{50}$ = 8.62 nmol/L) was isolated. In FZD1/2/7 knockout (FZD127-KO) 293T and HeLa cells, sF8_AG6 specifically blocked the FZD8 pathway without inhibiting the FZD5 pathway. However, although the development of sF8_AG6 provides insights into solving the specificity challenges, its anticancer efficacy and safety profile still require further validation through clinical trials.

Ge et al.[11] developed an epitope-directed antibody screening strategy. Because Site II in FZD proteins is less conserved than Site I, it serves as a key target for developing selective antibodies. Using F2. I and hB9L9.3 as antibody templates, Ge et al.[11] computationally analyzed their binding modes to Site II of the FZD1/2/7 CRD. hB9L9.3 exhibits similar interaction patterns with different FZD variants. Therefore, hB9L9.3 was selected for subsequent studies. On the one hand, researchers randomized the CDR residues of hB9L9.3 that interact with Site II to construct an antibody library. On the other hand, they generated a control antigen F7M1 to deplete non-specific binders. After five rounds of biopanning, an antibody named pF7_A5, which recognizes FZD1/2/7, was obtained. To further generate subtype-specific antibodies, Ge et al.[11] performed randomization on residues Y27, R28, and L95, which are involved in subtype-specific recognition. Employing the same control antigen strategy, they successfully isolated an FZD7-preferential antibody, sF7_A2, and an FZD2-specific antibody, sF2_C11 [11]. In the future, sF2_C11 can serve as a template for subsequent drug development.

### 5.3. *The limitations of FZD orthosteric inhibitors*

The CRD exhibits a high degree of evolutionary conservation among FZD family members. At the amino acid sequence level, the CRDs of different FZD subtypes show significant homology (Fig. 4A). For example, the highest sequence similarity among the FZD1/2/7 subfamilies can reach 80%. Even between FZD3 and FZD6, which share the lowest similarity, approximately 53% sequence identity is retained[181]. At the spatial conformation level, the CRD structures are highly superimposable[182] (Fig. 4B). The hydrophobic binding groove that accommodates the WNT PAM is nearly identical in its topological architecture. The dual conservation of sequence and structure collectively shapes a molecular recognition interface with extremely similar spatial topology and chemical microenvironment. This high degree of similarity physically and chemically limits the selectivity of FZD orthosteric inhibitors. When the CRDs of different FZD subtypes present nearly superimposable three-dimensional epitopes, the shape complementarity patterns between the inhibitor and these CRDs are highly similar. This spatial similarity leads to an averaging out of the short-range van der Waals interactions, preventing the generation of significant free energy differences when binding different subtypes[183]. Furthermore, the conservation of key binding residues further compromises specificity. Research indicates that the specificity of the nanobody Nb8, which binds the FZD3 CRD, is co-regulated by electrostatic complementarity, hydrogen bonding networks, and hydrophobic interactions[184]. Nb8 binds FZD3 with high affinity ($K_d \approx$ 19.2 nmol/L), but its binding to FZD6 is significantly weaker ($K_d \approx$ 1200 nmol/L). Its specificity originates from the hydrophobic residue M116, which is unique to FZD3. In contrast, the conserved residue K112 forms strong electrostatic attraction with the Nb8 surface, providing the basis for cross-reactivity[184]. In summary, the conservation of CRD make it easy for orthosteric inhibitors to form similar networks of non-covalent interactions with different FZD subtypes, which constitutes the core structural mechanism underlying their low targeting specificity.

Currently, all clinical trials involving OMP-18R5 have been terminated due to severe bone toxicity[28,185]. The primary reason is that its targets, FZD1/2/5/7/8, not only play pro-oncogenic roles but are also crucial for regulating normal bone tissue homeostasis. For example, FZD8 directly inhibits osteoclasts *via* the canonical WNT pathway[186]. FZD1 can promote osteoblast differentiation and mineralization[187]. FZD2 regulates limb development[188]. The broad pathway inhibition by OMP-18R5 directly impairs bone tissue homeostasis. Additionally, we analyzed other preclinical orthosteric inhibitors with publicly available epitope information. The results revealed that the key residue sites responsible for their activity exhibit high conservation (Fig. 4C). Therefore, the strategy of targeting CRDs to screen for high-affinity, highly selective ortho-inhibitors poses significant challenges in structure-based drug design. Moreover, it may lead to predictable adverse drug reactions.

In summary, orthosteric inhibition of FZD faces dual challenges from structural biology and clinical practice. Directly blocking the orthosteric functional site of FZD results in low selectivity and high toxicity. In contrast to orthosteric binding sites, allosteric binding sites typically endure less evolutionary pressure and may exhibit greater sequence diversity across different FZD subtypes[189]. More importantly, NAMs do not compete directly with endogenous WNT proteins or downstream signaling molecules for binding[190]. Instead, they regulate signaling pathways by altering the conformational state of these molecules. This non-complete-blocking mechanism can inhibit tumor-driving signals while preserving, to a greater extent, the physiological functions of receptors in normal tissues, such as bone homeostasis.

## 6. The NAMs that target FZD

NAMs represent a highly promising strategy for targeting FZD. They hold the potential to overcome the challenge of subtype selectivity posed by the highly conserved orthosteric binding sites. Furthermore, they offer novel ways for targeting the traditionally undruggable TMD of FZD. This section will first elaborate on the mechanisms and advantages of FZD NAMs. Then, we provide a systematic review of the reported FZD NAMs.

### 6.1. *The mechanism of NAMs*

FZD is a classic dynamically regulated system protein that achieves receptor activation or inactivation through conformational selection. When the CRD exposes its active site to WNT, specific conformations rearrange to form an active state that can be selectively recognized by DVL or G proteins[25]. Studies reveal that following endogenous ligand activation, FZD undergoes structural adjustments in its TMD. Most notably, TM6 swings outward,

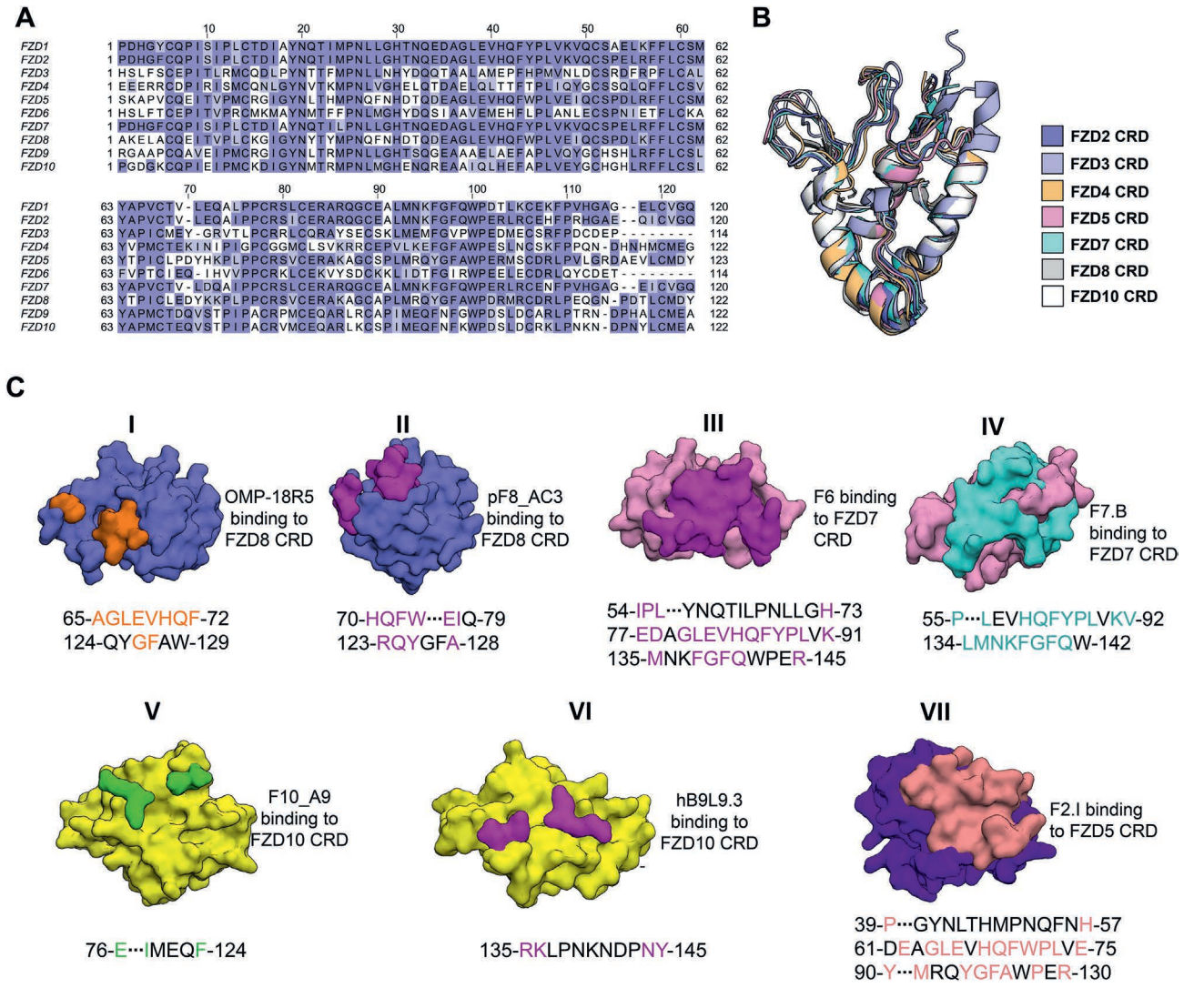


**Figure 4** The limitations of FZD orthosteric inhibitors. (A) Sequence alignment of the CRD from human FZD1-10. The amino acid sequences of ten FZD CRDs are highly conserved. (B) The CRD conformations of the FZD family are highly overlapping. Among them, the FZD2 CRD is in slate (PDB:7X8P). The FZD3 CRD is in light blue (PDB:8Q7O). The FZD4 CRD is in wheat (PDB:5CM4). The FZD5 CRD is pink (PDB:6O39). The FZD7 CRD is in cyan (PDB:5T44). The FZD8 CRD is in gray (PDB:8X0T). The FZD10 CRD is in white (PDB:7X8Q). (C) Antibody-interacting residues in the FZD CRD surface model. I. The residues (orange) of the FZD8 CRD (slate) participate in the interaction with OMP-18R5 (PDB:8X0T). The orange amino acid residues below represent the binding site. II. The residues (magenta) of the FZD8 CRD (slate) participate in the interaction with pF8_AC3 (PDB:8X0T). The magenta amino acid residues below represent the binding site. III. The residues (purple) of the FZD7 CRD (pink) participate in the interaction with F6 (PDB:5T44). The purple amino acid residues below represent the binding site. IV. The residues (cyan) of the FZD7 CRD (pink) participate in the interaction with F7. B (PDB:5T44). The cyan amino acid residues below represent the binding site. V. The residues (green) of the FZD10 CRD (yellow) participate in the interaction with F10_A9. The green amino acid residues below represent the binding site. VI. The residues (magenta) of the FZD10 CRD (yellow) participate in the interaction with hB9L9.3. The magenta amino acid residues below represent the binding site. VII. The residues (salmon) of the FZD5 CRD (purpleblue) participate in the interaction with F2.I. The salmon amino acid residues below represent the binding site. FZD (PDB:6O39).frizzled receptor; CRD, cysteine-rich domain.

opening the intracellular pocket. Following transducer protein binding, TM1, TM2, TM5, and TM7 slightly retract toward the receptor core, further stabilizing the active conformation[191] (Fig. 5). The rotational movements of the FZD helices are closely related to key residues. These critical residues are conserved across the FZD family. They mediate conformational changes in the receptor by forming and disrupting hydrophobic interactions and hydrogen bonds. Such residues are termed molecular switches[192]. Currently, multiple molecular switches have been identified through computational biology, molecular dynamics simulations, and cellular functional experiments (Fig. 5). Wright et al.[24] discovered that in the inactive state of FZD6, the side chain of $R^{6.32}$ forms stable hydrogen bonds and $\pi-\pi$ ionic stacking interactions with $W^{7.55}$. Disrupting the interaction network between $R^{6.32}$ and $W^{7.55}$ opens the intracellular pocket, leading to increased constitutive activity of FZD[24]. Study indicates that this molecular switch primarily functions as a negative regulator. It stabilizes FZD in its inactive state, limiting its transition to the

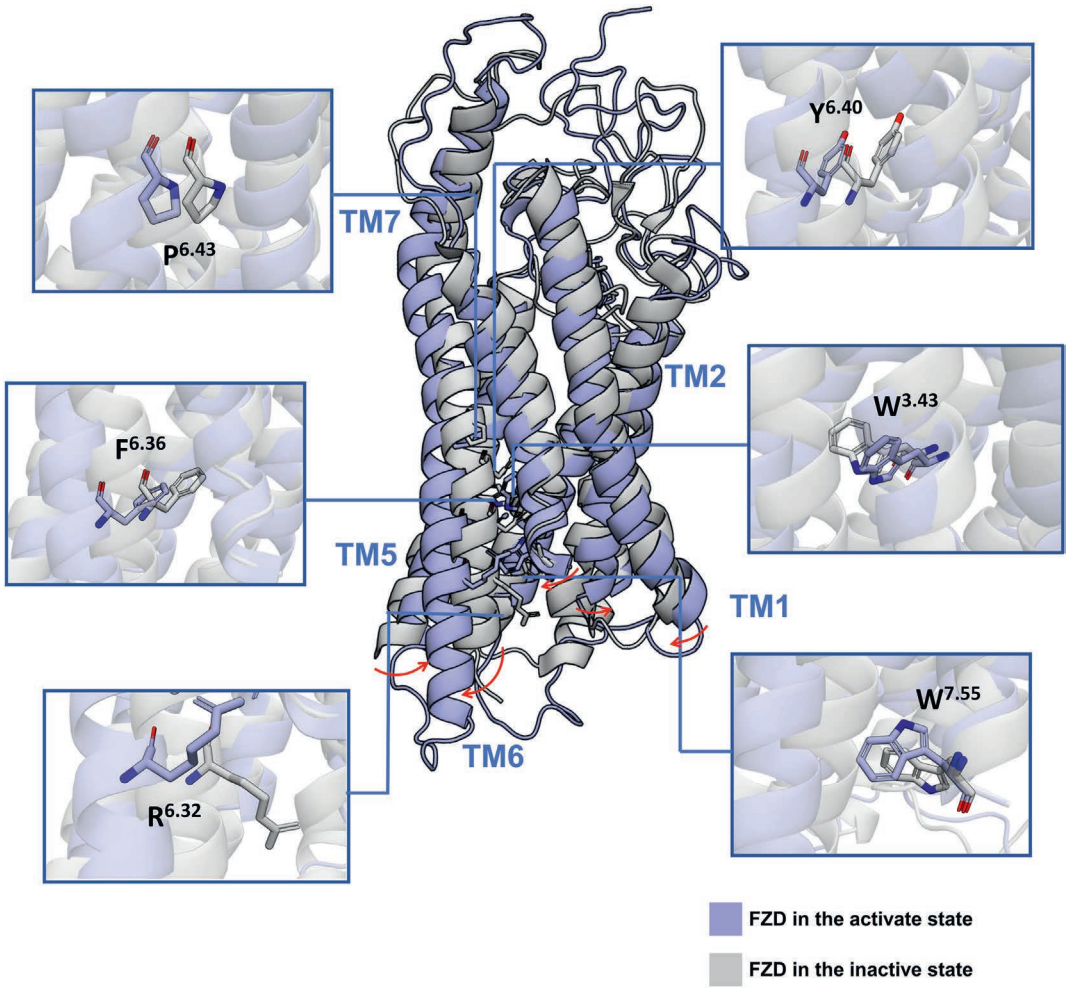


**Figure 5** The dynamic regulation mechanism of FZD. The slate-colored regions in the figure represent the activated state of FZD (PDB:6OT0). The gray regions indicate the inactive state of FZD (PDB:8JH7). The red arrows denote the direction of conformational change when FZD is activated. The boxes display the molecular switches. FZD, frizzled receptor; CRD, cysteine-rich domain.

active state. Subsequently, Turku et al.[193] extended this molecular switch to a larger aromatic network. The molecular switch between $R^{6.32}$ and $W^{7.55}$ connects to the kink $P^{6.43}$ in TM6 through an aromatic $\pi-\pi$ interaction network. In FZD, this network includes $Y^{6.40}$, $W^{3.43}$, $F^{6.36}$, and $W^{7.55,193}$.

The dynamic properties of FZD make it an ideal target for allosteric modulators. They stabilize receptors in different functional states by regulating conformational selection, thereby inducing differential responses to endogenous ligands[194]. NAMs constitute one class of allosteric modulators. Additionally, other allosteric modulators include positive allosteric modulators (PAMs), ago-PAMs, neutral allosteric ligands (NALs), and biased allosteric modulators (BAMs)[195]. NAMs reduce the affinity or efficacy of endogenous ligands, inhibiting signaling pathway activation. Conversely, PAMs enhance the affinity or efficacy of endogenous ligands[196]. Both PAMs and NAMs require the presence of an agonist ligand to exert their regulatory effects (Fig. 6A). As of now, FZD NAMs account for 8% of FZD modulators. FZD PAMs account for 4%. FZD orthosteric inhibitors remain the primary class of FZD modulators, comprising 60%. FZD orthosteric agonists that directly bind to the WNT binding site in the CRD to activate FZD account for 12% (Fig. 6B)[197].

Mechanistically, NAMs regulate the endogenous ligand–receptor complex through diverse mechanisms. NAMs can inhibit receptor binding to signal transduction proteins by stabilizing the inactive conformation[198,199]. Among these, interactions affecting molecular switches can stabilize the conformation toward the inactive state. For example, $I124^{3.40}$, $P214^{5.50}$, and $F251^{6.44}$ are molecular switches in the C5a receptor[200]. In the inactive state, they form a hydrophobic structural region. This helps maintain the inactive conformation of C5aR. Avacopan and NDT9513727 are NAMs of the C5a receptor[200]. They can form hydrophobic interactions with these residues. This stabilization prevents the rotation and outward movement of TM5 and TM6 required during activation, thereby inhibiting receptor activation[200]. Since the aforementioned molecular switches are conserved across various GPCR families, similar mechanisms have been reported for NAMs of the $\beta_2$ adrenergic receptor[201]. Molecular switches including $P211^{5.50}$, $I121^{3.40}$, $F282^{6.44}$, and $E122^{3.41}$. They constitute a conserved conformational regulatory hub in the $\beta_2$ adrenergic receptor. AS408, the $\beta_2$ adrenergic receptor NAM, stabilizes the inactive conformation of these residues through hydrogen bonding with $E122^{3.41}$ and hydrophobic interactions[201]. This directly inhibits the conformational transition of the $\beta_2$ adrenergic receptor.

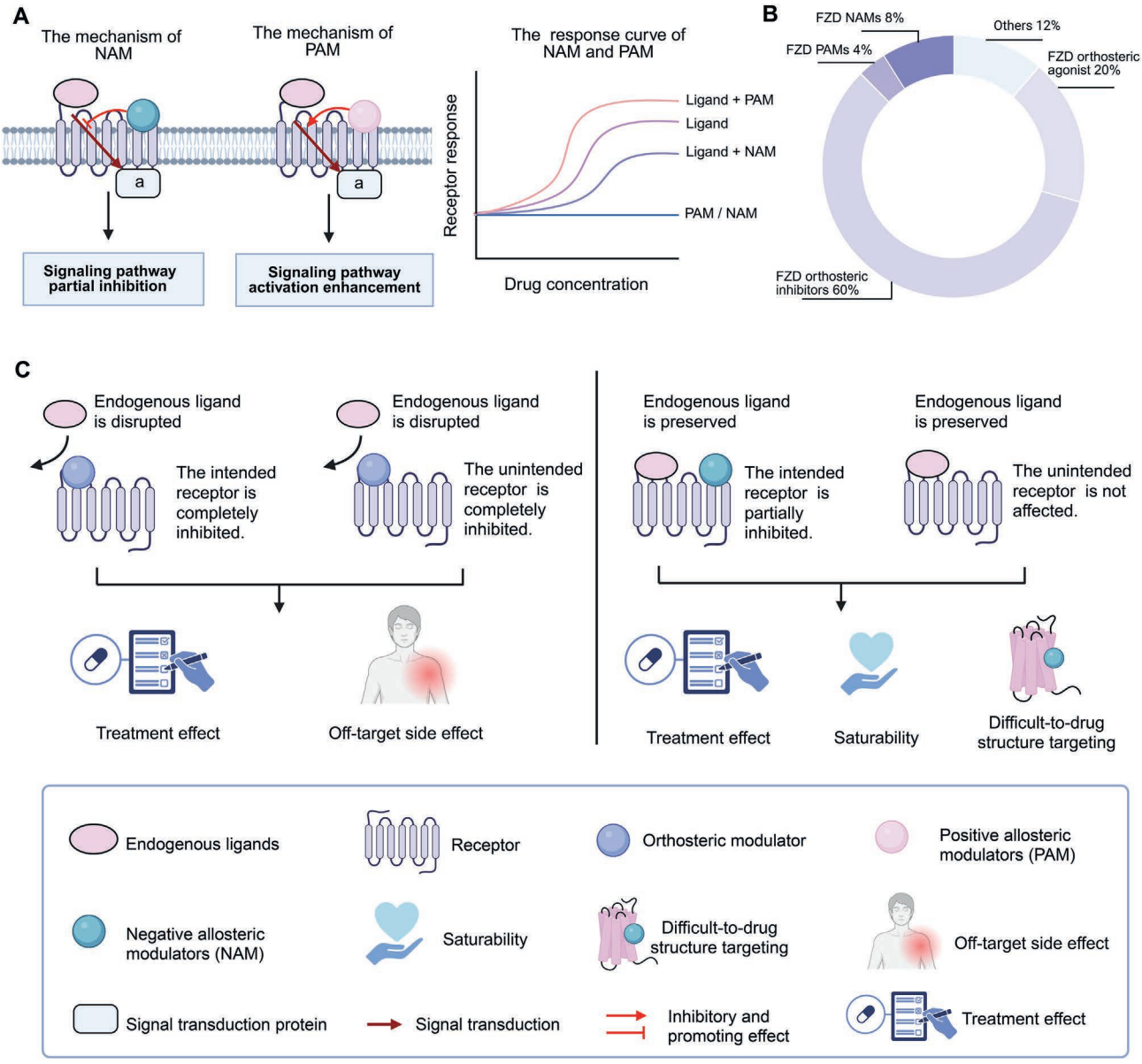


**Figure 6** The mechanism of NAMs. (A) Comparison of the pharmacological mechanisms between NAMs and PAMs. NAMs partially inhibit signaling pathway activity. PAMs enhance receptor activation. The right panel illustrates the differential effects of drug concentration on receptor response. It highlights the saturable, non-competitive regulatory properties of NAMs and PAMs. (B) The pie chart summarizes the current landscape of drug tools targeting FZD receptors. Orthosteric inhibitors constitute the majority (60%). Orthosteric agonists account for 20%. Allosteric modulators represent a smaller proportion: FZD NAMs account for 8%, while FZD PAMs constitute only 4%, highlighting the untapped potential of this receptor category in allosteric targeting. Other drug classes comprise 12%. (C) Advantages of FZD NAMs over FZD orthosteric inhibitors. Traditional orthosteric inhibition often results in complete receptor blockade, which disrupts endogenous ligand homeostasis. This can lead to intended treatment effects but also cause off-target side effects *via* unintended, complete inhibition of related pathways. In contrast, NAMs preserve endogenous ligand signaling while providing partial, saturable inhibition of the intended receptor. This approach spares the unintended receptor, minimizes pathway-wide disruption, and enables difficult-to-drug structure targeting through novel binding sites. FZD, frizzled receptor; NAM, negative allosteric modulator; PAM, positive allosteric modulator.

Additionally, some NAMs can stabilize inactive conformations by acting as molecular glue. Specifically, SHP099 is a NAM of SHP2 protein[202]. In its resting state, the N-terminal SH2 domain (N-SH2) of the SHP2 protein autoinhibits the catalytic active site of its protein tyrosine phosphatase (PTP) domain. This maintains SHP2 in an autoinhibited conformation. When bis-phosphorylated peptides are present, they bind simultaneously to both the N-SH2 and C-SH2 domains, inducing a conformational change[202]. This releases the N-SH2 domain from the active site, thereby activating SHP2. SHP099 binds to the central tunnel formed at the interface of the N-SH2, C-SH2, and PTP domains, locking SHP2 in its autoinhibited conformation through hydrogen bonding and hydrophobic interactions. Consequently, it blocks the downstream RAS−ERK signaling pathway and inhibits tumor cell growth[202]. NAMs can also prevent the rotation of molecular helices by forming steric hindrance. This also leads to the inability to form the

active conformation[203,204]. It has been reported that lipophilic NAMs enter the intracellular region of the target, preventing receptor binding to signal transduction proteins[205]. This lipophilic vericiron binds inside the transmembrane helix bundle of the CCR9 receptor. It forms steric hindrance in the intracellular region, causing steric clashes with the presumed binding sites of G proteins[205]. Notably, the mechanism of action of allosteric modulators exhibits probe dependency. This manifests as the regulatory effect of allosteric modulators varying with different endogenous ligands[206]. This primarily occurs because different endogenous ligands can induce distinct conformations in the receptor[206]. Therefore, during drug development, the effects of all possible allosteric modulators should be evaluated under various endogenous ligands. This will effectively prevent clinical trial failures.

Compared to orthosteric inhibitors, NAMs offer several advantages (Fig. 6C). First, they possess greater potential for drug targeting specificity. Due to lower evolutionary pressure on allosteric binding sites, their residues exhibit lower conservation[207]. When targeting the highly conserved FZD family, NAMs may more precisely target a specific FZD subtype. This helps reduce the occurrence of adverse reactions such as bone toxicity. Second, due to the synergistic interaction between endogenous ligands and NAMs, the efficacy of NAMs can reach a saturable limit[208]. This effectively controls the severity of adverse reactions caused by drug overdose or off-target effects. Third, NAMs require endogenous ligands to bind to receptors to exert regulatory effects. Consequently, they synergistically enhance or inhibit signaling only when endogenous ligands are released within specific spatiotemporal windows[209,210]. This mode of action offers dual advantages: on one hand, its effects align with the spatiotemporal rhythms and steady-state conditions of physiological signaling; on the other hand, elevated endogenous ligand levels in specific regions can enhance receptor sensitivity to NAMs, enabling tissue- or pathway-specific interventions. Finally, NAMs provide novel ways for targeting the traditionally undruggable TMD region of FZD[211]. NAMs avoid direct competition at the interface between endogenous ligands and receptors. By binding to spatially distinct allosteric sites, they achieve fine-tuned modulation of protein function. Furthermore, even when no obvious pockets are visible in static crystal structures, rational drug design can leverage dynamic conformational changes by capturing concealed allosteric pockets exposed in intermediate or excited states[212].

### 6.2. *Current situation of FZD NAMs*

Currently, researchers have identified a series of small-molecule and peptide NAMs. The development of NAMs targeting FZD has achieved a series of advancements. Drug development primarily focuses on three structural domains: the CRD, the 7TMD, and the ICL3. Below, we will systematically introduce these FZD NAMs.

#### 6.2.1. *C407*

FZD7 exhibits structural similarity to the SMO receptor within the same family. Using four distinct ligand-bound structures of SMO (PDB: 6XBL; 4O9R; 5L7I; 4N4W), Scharf et al.[30] constructed four different docking models. These models simulated the binding poses of potential ligands at various depths within the TMD of FZD7. Subsequently, a large-scale virtual screening was conducted, leading to the preliminary identification of the hit compound C45. Due to C45's low $pIC_{50}$, researchers used it as a starting point to discover the more promising compound C407 and a series of its structural analogs. This process revealed a crucial pharmacophore scaffold, 5-methyl-3*H*-thieno[2,3-*d*] pyrimidin-4-one[30]. C407 was proven to interfere with the conformational rearrangement between FZD7 and DVL, thereby inhibiting WNT3A-induced $\beta$-catenin signaling activation[30]. C407 is a potential NAM of FZD7. More importantly, researchers elucidated the dynamic binding trajectory of C407. C407 moves from its initial virtual docking site deeper into the 7TMD, forming polar interactions with residues $S351^{3.40}$ and $Y489^{6.51}$ (Fig. 7A). During this descent, C407's fluorophenyl moiety inserts between the receptor's TM3 and TM6 domains. This specifically disrupts the conserved molecular switch network, thereby maintaining FZD7 in a non-activated state[30].

However, due to the conservation of the targeted site across the FZD family, C407's subtype selectivity falls short of expectations. Furthermore, its inhibitory potency ($pIC_{50} = 4.86 \pm 0.04$) remains relatively low[30]. Structure-based rational optimization for subtype selectivity and inhibitor potency is still required. For instance, modifying the amide side chain could enhance interactions with $Ser351^{3.40}$. Altering peripheral groups around the core scaffold to explore less conserved regions within 7TMD. This may enhance efficacy and subtype selectivity. Furthermore, the established strategy targeting allosteric cavities can be extended to NAMs of other members of the FZD family.

#### 6.2.2. *FzM1*

Chaperone molecules are small molecules that specifically stabilize the conformation of target proteins, thereby promoting their correct folding, transport, and restoration of function[213]. Thus, drug-folding chaperones may serve as specific binding ligands for receptors. Based on this strategy, researchers discovered a small-molecule NAM targeting FZD4[32]. They employed the FZD4 mutant causing FEVR (FZD4-FEVR) as a screening platform. By assessing compounds' ability to restore FZD4-FEVR's proper folding and membrane localization, they identified the lead compound FzM1[32]. FzM1 effectively binds to FZD4, inhibiting Norrin-induced activation of the Wnt/$\beta$-catenin signaling pathway. The binding site of FzM1 was precisely localized to the ICL3 region of FZD4, specifically near residues S418 and T425. This region constitutes the critical interface for FZD4−DVL interaction. Following FzM1 binding to ICL3, the solvent accessibility of ICL3, TM5-7, and the C-terminal tail was significantly reduced. This indicates that ligand binding induces conformational tightening in these regions, thereby disrupting the effective recruitment of DVL[32]. In the GBM cell line U87MG and the colorectal cancer cell line CaCo-2, FzM1 treatment suppressed the expression of tumor cell stemness markers, neurosphere formation, and migration capacity, demonstrating its antitumor potential as an NAM of FZD4[32].

Although FzM1's binding specificity remains unvalidated, the ICL3 sequence is highly conserved across ten FZD receptors. Consequently, FzM1 may still cross-activate other FZDs. Furthermore, S418 is similarly conserved in SMO[32]. Therefore, future efforts should focus on developing highly specific FZD NAMs based on the FzM1 lead compound scaffold. Overall, this folding rescue-based small molecule drug screening strategy offers a novel approach for inhibitor development. The C-terminal tail of FZD4-FEVR can be fused as a universal aggregation tag to other target proteins, enabling the artificial creation of folding-defect variants for screening.

#### 6.2.3. *dFz7-21*

Using phage display technology, researchers screened for the peptide inhibitor Fz7-21, which binds to the FZD7 CRD[33]. In

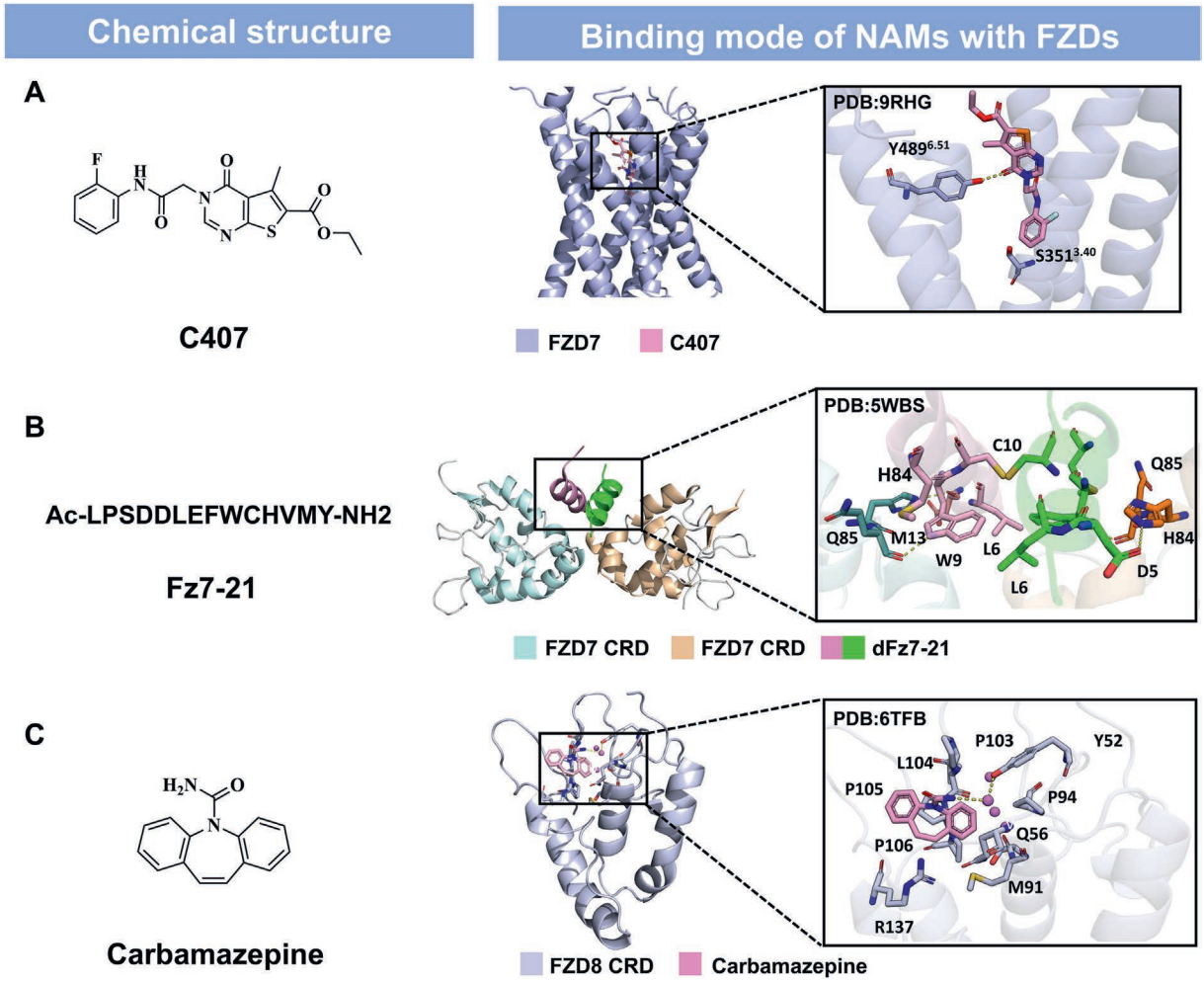


**Figure 7** The FZD NAMs. (A) The left side shows the chemical structure of C407, while the right side depicts the model of C407 and FZD7 in combination (PDB:9RHG). FZD7 is represented in slate. C407 is shown in pink. (B) The chemical structure of Fz7-21 is shown on the left. Binding mode of its dimer, dFz7-21, with the FZD7 CRD is on the right (PDB:5WBS). FZD7 CRD is represented in wheat and palecyan. dFz7-21 is shown in pink and green. (C) The left panel shows the chemical structure of carbamazepine. The right panel depicts the binding mode of carbamazepine with FZD8 CRD (PDB:6TFB). FZD8 CRD is represented in light blue. Carbamazepine is shown in pink. FZD, frizzled receptor; CRD, cysteine-rich domain; NAM, negative allosteric modulator.

HEK293 cells, Fz7-21 inhibited WNT3A-induced $\beta$-catenin signaling with an $IC_{50}$ of approximately 100 nmol/L. Subsequently, researchers converted Fz7-21 into the homodimer dFz7-21 *via* chemical oxidation. The $IC_{50}$ of dFz7-21 increased to approximately 2.5 nmol/L, with picomolar affinity for the FZD7 CRD ($K_d$ = 3 nmol/L)[33]. dFz7-21 binds at the apex of the FZD7 CRD dimer interface. This position is adjacent to but does not directly block the opening of the lipid-binding groove, representing a novel, previously uncharacterized binding site. Specifically, the L6 residue of dFz7-21 inserts into a hydrophobic pocket[33]. The main-chain carbonyl of dFz7-21's D5 forms a hydrogen bond with the side chain of H84 on the other CRD monomer. The indole nitrogen of W9 forms another critical hydrogen bond with the main-chain carbonyl of Q85. Together, these constitute a precise polar anchoring network. Additionally, the side chain of M13 interacts with the surrounding hydrophobic environment *via* van der Waals forces, further stabilizing the binding[33] (Fig. 7B). Interestingly, dFz7-21 acts like a lid, inducing a relative rotation of approximately 75° in the CRD dimer. This causes the lipid-binding groove to transform from a bent U-shaped conformation to an open, extended state. This dramatic conformational rearrangement maintains the FZD7 CRD in an inactive state. Experiments demonstrate that dFz7-21 does not prevent purified WNT3A from binding to the FZD7 CRD, but rather inhibits the formation of the WNT-FZD-LRP6 ternary complex[33]. This complex is essential for activating downstream $\beta$-catenin signaling. dFz7-21 exhibits high selectivity[33]. Leveraging the resolved high-resolution complex structure, future structure-based virtual screening and optimization targeting specific sites of dFz7-21 hold promise for developing highly selective FZD inhibitors that bind to the same allosteric pocket.

#### *6.2.4. Carbamazepine*

Zhao et al.[35] reported the crystal structure of the anti-epileptic drug carbamazepine bound to the CRD of FZD8 (Fig. 7C). Notably, carbamazepine exhibits remarkable subtype selectivity. Surface plasmon resonance screening revealed that carbamazepine specifically binds to the FZD8 CRD ($K_d$ = 17 μmol/L). Carbamazepine does not bind to the FZD5 CRD, despite its over 80% sequence homology with FZD8. This selectivity is primarily

determined by the unique Y52 residue in FZD8. This residue corresponds to H50 in FZD5[35]. This single-amino-acid-based targeting specificity provides crucial structural information for designing highly selective NAMs. Mechanistically, carbamazepine binds to an unreported hydrophobic pocket within the FZD8 CRD. This pocket lies between the known WNT and FZD binding sites and is primarily composed of residues from $\alpha$3-helix, loop 2, loop 4, and loop 6[35]. Four proline residues (P94, P103, P105, P106) form a unique hydrophobic cluster that serves as the core scaffold stabilizing carbamazepine. The dibenzazepine ring and the two benzene rings of carbamazepine form extensive van der Waals interactions with residues in the pocket, such as P105, P103, L104, and M91 [35]. Meanwhile, the phenolic hydroxyl group of Y52 in FZD8 forms an indirect hydrogen bond network with the nitrogen atom of the carbamazepine amide group *via* a highly ordered structural water molecule. Interestingly, carbamazepine binding exerts a specific stabilizing effect on the receptor conformation. In the apo structure, loop 6, which is responsible for WNT binding, exists in two conformations, a and b[35]. However, in the carbamazepine complex, loop 6 is locked exclusively in the b conformation. In the known WNT8/FZD8 complex structures, WNT prefers to bind FZD8 when its loop 6 is in the a conformation. Therefore, carbamazepine stabilizes a receptor conformation that is unfavorable for WNT binding. This partially interferes with the binding of WNT proteins to the FZD8 CRD, explaining its partial blockade of WNT signaling.

Cellular assay data show that even at concentrations as high as 64 μmol/L, carbamazepine only inhibits WNT3A-induced reporter gene activation by approximately 40%[35]. Consequently, fine-tuning the strength of WNT signaling rather than completely blocking the pathway may offer greater safety potential. Moreover, carbamazepine's favorable subtype selectivity makes it a lead compound template for developing new FZD NAMs. However, the micromolar-level weak binding of carbamazepine may pose an off-target risk. In the future, SAR studies based on the water molecule network and hydrophobic interactions are still needed to improve its affinity. Furthermore, the structural model studies the complex of the isolated CRD with carbamazepine, not the full-length FZD8 receptor in a membrane environment. Conformational coupling between the CRD and the 7TMD cannot be captured in this model. The crystal structure of full-length FZD8 bound to carbamazepine still needs to be resolved.

## 7. Challenges and prospects of FZD NAMs

Currently, the application of FZD NAMs has both challenges and prospects. On the one hand, the number of available FZD NAMs remains limited. Their development faces multiple challenges. On the other hand, combining FZD NAMs with conventional chemotherapy, radiotherapy, and immunotherapy holds promise in overcoming treatment resistance and enhancing therapeutic efficacy.

### *7.1. Design and development of FZD NAMs*

Currently, the development of FZD NAMs still lacks high-resolution structural insights and predictive platforms for selective design. This severely limits the progress of drug development. Furthermore, existing NAMs still exhibit issues such as insufficient potency and affinity. Therefore, there is an urgent need to establish a standardized and efficient development workflow for NAMs. Presently, experimental methods and computational approaches constitute the primary strategies for NAM discovery[208].

#### *7.1.1. Computational and structural biology for the development of FZD NAMs*

Computational biology plays an increasingly vital role in the development of NAMs by integrating computational simulations, data mining, and biology[214]. Its core advantage lies in steering the development of NAMs from serendipitous discovery toward rational design. This significantly reduces research costs and timelines. The modular development process of computational biology is primarily reflected in the accurate prediction of allosteric sites; virtual screening of potential NAMs; and simulating the mechanism of drug binding[215]. Among these, predicting allosteric sites is the most critical step in structure-based drug development. Consequently, researchers primarily focus on developing and optimizing computational methods for this aspect. Currently, machine learning approaches represent the main research direction[216]. The Allosteric Database (ASD) serves as the primary dataset for machine training[217]. ASD's structural data originates from both experimental measurements *via* X-ray crystallography and NMR, as well as structural predictions from AI tools like AlphaFold[218]. As of 2023, ASD has systematically cataloged 2422 allosteric protein structures, 3102 ligand−protein complex structures, and 66,589 potential allosteric sites[218]. Furthermore, ASBench and CASBench are also derivative datasets of ASD[218]. Traditional supervised prediction models include Random Forest, Support Vector Machines (SVM), and XGBoost [219-221]. For example, the SVM is a learning classification algorithm used for allosteric site prediction. Its core mechanism involves extracting 21 key descriptors from protein structures as input feature vectors. It then seeks an optimal separating hyperplane to distinguish allosteric sites from non-allosteric sites[222]. In recent years, prediction models have gradually shifted towards deep neural networks, including Graph Neural Networks (GNNs) and Protein Language Models (PLMs) [223-225]. Zhu et al.[226] proposed integrating a GNN-based Neural Relational Inference (NRI) model with molecular dynamics simulations to uncover long-range allosteric interaction pathways and dynamic signal transduction mechanisms in proteins. This model can automatically infer potential interaction networks between residues from relatively short simulation times. It also outperforms traditional methods in predicting free energy changes induced by mutations[226]. The performance of PLMs in predicting allosteric sites is promising, primarily drawing on concepts from natural language processing[227]. PLMs treat sequences as a biological language, leveraging large-scale sequence data to mine evolutionary patterns and spatial features. Models like ESMfold, based on the pre-trained PLM ESM-2, can rapidly and accurately predict protein three-dimensional structures from sequence alone[227]. Currently, annotated allosteric sequence data for training is still insufficient, but ESM-2 has demonstrated the ability to identify correlations among allosteric residues. Therefore, it holds significant potential for allosteric site prediction[227]. However, despite progress in machine learning models, the prediction accuracy of various models like PASSerRank and AllositePro remains below 60%[228,229]. One reason is that current training data is often limited to certain protein families, causing models to potentially overfit to local features specific to those families. The prediction models fail to learn features or evolutionary patterns common to all allosteric sites[228,229]. Therefore, overcoming data limitations and expanding model applicability is crucial for improving machine learning

methods. Furthermore, the lack of high-quality protein structures and annotated allosteric sequence data also limits the accuracy of allosteric site prediction. In the future, data quality enhancement through AI models like ESM-2 or experimental methods is necessary[218].

Structural biology primarily focuses on resolving the structures of NAMs and their receptors; elucidating the mechanisms of allosteric modulation; and providing high-quality allosteric data for proteins. X-ray crystallography stands as one of the most prevalent experimental methods within structural biology. This technique involves irradiating ordered crystals formed by biological macromolecules with X-rays. Subsequently, by analyzing the resulting diffraction patterns, the three-dimensional structure within the molecule is determined[230]. X-ray crystallography plays a crucial role in structure-based drug design for identifying allosteric binding pockets. For instance, Wang et al.[231] employed X-ray crystallography to resolve the complex structure of the human P2X3 receptor bound to the NAM AF-219. This reveals a negative allosteric site located between adjacent subunits. Structural analysis indicated that AF-219 partially embeds into this site *via* hydrophobic interactions and hydrogen bonds. Its binding inhibits channel opening through conformational changes[231]. This atomic-level structure not only elucidates the inhibition mechanism of the P2X3 receptor, but also provides a critical structural foundation for designing subtype-specific allosteric drugs. Cryo-EM, which serves a similar function, is also playing an increasingly important role in the development of NAMs. Cryo-EM determines the structures of biological macromolecules and their complexes by flash-freezing samples in vitreous ice[232]. Its advantage lies in preserving their native conformations and interactions as in aqueous solution. Cryo-EM is particularly important for resolving the complex three-dimensional structures and activation mechanisms of FZD receptors[233]. It is noteworthy that neither cryo-EM nor X-ray crystallography can directly capture a continuous picture of protein dynamic regulation. Therefore, their application in studying allosteric regulatory mechanisms may be limited. In contrast, NMR spectroscopy can quantitatively characterize dynamic processes such as conformational changes and ligand binding across timescales from picoseconds to milliseconds[234]. NMR is sensitive enough to capture even transiently populated, low-abundance conformational states[235].

#### *7.1.2. The challenges in developing FZD NAMs*

First, NAMs may exhibit inconsistencies between binding affinity and functional effects. The complexity of drug development lies in the fact that NAMs may enhance the binding affinity of endogenous ligands while simultaneously inhibiting signaling efficacy[236,237]. For example, the NAM Org27569 stabilizes the CB1 receptor in an inactive conformation, yet concurrently increases the agonist's binding affinity[238]. Therefore, optimizing lead compounds based on SAR requires concurrent evaluation using both binding assays and functional assays. Secondly, NAMs may exhibit an induced-fit characteristic when binding to their target receptors[239]. This means their binding necessitates inducing local or global conformational rearrangements in the receptor to form a complementary binding interface. For many NAMs, entering the pocket and inducing conformational change requires overcoming a significant energy barrier[239]. Consequently, the modulator must not sterically clash with the receptor's transition state or final bound conformation. Minor chemical modifications can disrupt the ability to induce the conformational change and fail to maintain key interactions within the induced pocket. Third, NAMs typically exhibit lower affinity and may fail to lock receptors into a single stable conformation as effectively as orthosteric inhibitors[240]. This results in poor crystallographic order, making it challenging to obtain high-quality co-crystal structures of complexes. Furthermore, some NAMs are polyaromatic or highly lipophilic, making it difficult to obtain homogeneous aqueous solutions suitable for crystallization[240]. Fourth, some NAMs exhibit slow binding or dissociation kinetics[241]. This may relate to the binding and dissociation processes constrained by the slow steps of receptor conformational change. In terms of pharmacodynamics, a slow dissociation rate can lead to a prolonged duration of action, reducing dosing frequency. However, it may also result in irreversible inhibition, making it difficult to rapidly reverse effects in case of adverse reactions[241].

### *7.2. FZD NAMs combined with other therapies*

Radiation therapy and chemotherapy remain the traditional approaches in cancer treatment[242]. Mechanistically, radiation therapy induces DNA damage through ionizing radiation, triggering apoptosis in cancer cells. Chemotherapy drugs such as cisplatin and paclitaxel inhibit tumor growth by interfering with DNA synthesis and microtubule function[243]. However, despite continuous advancements in chemotherapy and radiation therapy, drug resistance remains the primary cause of treatment failure and cancer recurrence[244]. Combining inhibitors targeting key resistance nodes with radiotherapy and chemotherapy has emerged as a critical strategy[244]. Compared to traditional targeted therapies, NAMs selectively eliminate tumor cells dependent on specific molecular subtypes while sparing normal tissues. In clinical trials, combination therapy with NAMs shows promise in mitigating dose-limiting toxicities. Currently, combinations of FZD NAMs with chemotherapy have been reported. For instance, in TNBC, activation of the FZD7-mediated Wnt/$\beta$-catenin signaling pathway drives carboplatin resistance. Cai et al.[102] employed Fz7-21 to inhibit Wnt/$\beta$-catenin signaling activation, thereby significantly reducing CSC self-renewal and tumor initiation capacity. Concurrently, Fz7-21 significantly enhances carboplatin sensitivity in TNBC by disrupting homologous recombination repair mechanisms. Combining Fz7-21 with carboplatin markedly suppressed tumor growth and reduced lymph node metastasis. This demonstrates its potential as a therapeutic strategy targeting FZD7 to overcome chemotherapy resistance[102].

Immunotherapy, particularly immune checkpoint inhibitors, is a treatment method that activates the patient's own immune system to recognize and attack cancer cells. Among these, the most common immune checkpoints are PD-1/PD-L1 and CTLA-4[245]. Although immunotherapy has shown therapeutic potential in various cancers, a considerable proportion of patients still experience primary or acquired resistance. The tumor immunosuppressive microenvironment, which is regulated by signaling pathways, is one of the main causes leading to immunotherapy resistance. Therefore, the synergistic effect of targeting core molecules in these pathways with immunotherapy is expected to improve the efficacy of cancer treatment[246]. Among these strategies, NAMs offer higher target specificity and tissue selectivity, which can reduce toxicity to normal cells and lower the risk of off-target effects in combination therapies. Furthermore, due to the saturability of their efficacy, they hold potential in avoiding immune system overactivation-induced exhaustion or cytokine storms. Studies have shown that targeting the FZD-mediated WNT signaling pathway in combination with anti-PD1 therapy successfully reshapes the immunosuppressive tumor

microenvironment[247]. But research on the combination of FZD NAMs with immunotherapy is still currently lacking. In the future, it will be necessary to evaluate the therapeutic efficacy of combining FZD NAMs with immunotherapy across different cancers.

## 8. Conclusions

For clinical applications, we aim to develop inhibitors of the WNT signaling pathway to achieve favorable therapeutic outcomes. However, due to the pathway's extensive involvement in physiological processes, the use of non-selective inhibitors such as porcupine and tankyrase inhibitors is limited[248,249]. This constraint has shifted focus toward FZD proteins as therapeutic targets. As a key molecule in the WNT signaling pathway, FZD plays an extremely important role in cancer initiation and progression[250]. Therefore, targeting FZD has become a new strategy for anticancer therapy. The development of FZD orthosteric inhibitors has been ongoing for nearly 20 years. Progress has advanced from the first FZD10 antibody to the first antibody, OMP-18R5, entering clinical trials, and subsequently to antibody designs targeting specific FZD sites. However, to date, no FZD orthosteric inhibitor has successfully reached the market. The primary reason lies in the highly conserved sequences and similar structures within the FZD family. Distinguishing between different FZD subtypes has become a major obstacle in drug development.

With advances in Cryo-EM, molecular dynamics simulations, and structure-based mutagenesis studies, significant progress has been made in understanding FZD structures and activation mechanisms. On the one hand, cryo-EM has successfully resolved high-resolution three-dimensional structures of several FZD receptors bound to ligands. These structures clearly illustrate how the CRD of FZD precisely recognizes and binds ligands[22]. More importantly, these structures reveal that FZD undergoes significant conformational rearrangement upon signal complex activation. This provides direct evidence for understanding the mechanism of its allosteric effects. On the other hand, the discovery of molecular switches offers a microscopic perspective on the dynamic regulatory mechanism. Furthermore, in drug design and development, NAMs can achieve conformational selection regulation by altering the conformational dynamics of molecular switches[30]. Currently, the resolved FZD structures and molecular regulatory mechanisms are rapidly translating into potential clinical applications.

NAMs represent one of the most promising strategies for targeting FZD receptors. This approach enables more precise regulation of receptor function and may offer enhanced selectivity[204]. NAMs selectively target non-conservative allosteric binding sites on specific FZD subtypes. This enables NAMs to selectively inhibit individual dysregulated receptors without affecting others[251]. This is crucial for treating cancers driven by the upregulation of specific FZD receptors. Furthermore, NAMs exhibit superior pharmacological properties by modulating FZD affinity for WNT ligands. This precise control can mitigate the mechanistic toxicity associated with complete pathway blockade. However, translating this strategy into clinical applications still requires future systematic research. Among these challenges is the discovery of novel allosteric sites. Current efforts remain largely serendipitous. The integration of structural biology and computational biology is likely to be a critical approach for the future development of FZD NAMs.

## Acknowledgments

This work was supported by grants from the National Natural Science Foundation of China (82472686 and 82273320), and Research and Development Program, West China Hospital of Stomatology Sichuan University (RD-03-202505).

## Author contributions

Jing Li and Jiantang Yang conceived the study and revised the manuscript. Jiaqi Liang and Yiming Pan retrieved the related literatures and wrote the manuscript. Jiaqi Liang and Zhenyu Kong created the pictures and produced the tables. Boyang Wang revised the manuscript. All authors have read and approved this version of manuscript.

## Conflicts of interest

The authors declare that there are no conflicts of interest.

## References

1. Wu X, Que H, Li Q, Wei X. Wnt/$\beta$-catenin mediated signaling pathways in cancer: recent advances, and applications in cancer therapy. *Mol Cancer* 2025;**24**:171.
2. Song P, Gao Z, Bao Y, Chen L, Huang Y, Liu Y, et al. Wnt/$\beta$-catenin signaling pathway in carcinogenesis and cancer therapy. *J Hematol Oncol* 2024;**17**:46.
3. Liang J, Pan Y, Yang J, Zeng D, Li J. WNT signaling in cancer: molecular mechanisms and potential therapies. *Mol Biomed* 2025;**6**:83.
4. Zhou Y, Xu J, Luo H, Meng X, Chen M, Zhu D. Wnt signaling pathway in cancer immunotherapy. *Cancer Lett* 2022;**525**:84−96.
5. Chen Y, Chen Z, Tang Y, Xiao Q. The involvement of noncanonical Wnt signaling in cancers. *Biomed Pharmacother* 2021;**133**:110946.
6. Sutkeviciute I, Vilardaga JP. Structural insights into emergent signaling modes of G protein-coupled receptors. *J Biol Chem* 2020;**295**:11626−42.
7. Hilger D, Masureel M, Kobilka BK. Structure and dynamics of GPCR signaling complexes. *Nat Struct Mol Biol* 2018;**25**:4−12.
8. Mohr K, Schmitz J, Schrage R, Tränkle C, Holzgrabe U. Molecular alliance-from orthosteric and allosteric ligands to dualsteric/bitopic agonists at G protein coupled receptors. *Angew Chem Int Ed Engl* 2013;**52**:508−16.
9. Gurney A, Axelrod F, Bond CJ, Cain J, Chartier C, Donigan L, et al. Wnt pathway inhibition *via* the targeting of Frizzled receptors results in decreased growth and tumorigenicity of human tumors. *Proc Natl Acad Sci U S A* 2012;**109**:11717−22.
10. Liu HY, Sun XJ, Xiu SY, Zhang XY, Wang ZQ, Gu YL, et al. Frizzled receptors (FZDs) in Wnt signaling: potential therapeutic targets for human cancers. *Acta Pharmacol Sin* 2024;**45**:1556−70.
11. Ge Q, Teng M, Li X, Guo Q, Tao Y. An epitope-directed selection strategy facilitating the identification of Frizzled receptor selective antibodies. *Structure* 2023;**31**:33−43.e5.
12. Canals M, Sexton PM, Christopoulos A. Allostery in GPCRs: 'MWC' revisited. *Trends Biochem Sci* 2011;**36**:663−72.
13. Zhu C, Lan X, Wei Z, Yu J, Zhang J. Allosteric modulation of G protein-coupled receptors as a novel therapeutic strategy in neuropathic pain. *Acta Pharm Sin B* 2024;**14**:67−86.
14. Mandai T, Simen AA, Laurenza A, Kimura H. M1 receptor positive allosteric modulators discovery approaches. *Trends Pharmacol Sci* 2025;**46**:298−302.
15. Bian Y, Jun JJ, Cuyler J, Xie XQ. Covalent allosteric modulation: an emerging strategy for GPCRs drug discovery. *Eur J Med Chem* 2020;**206**:112690.

16. Gubb D, García-Bellido A. A genetic analysis of the determination of cuticular polarity during development in Drosophila melanogaster. *J Embryol Exp Morphol* 1982;**68**:37−57.
17. Vinson CR, Conover S, Adler PN. A Drosophila tissue polarity locus encodes a protein containing seven potential transmembrane domains. *Nature* 1989;**338**:263−4.
18. Adler PN, Vinson C, Park WJ, Conover S, Klein L. Molecular structure of frizzled, a Drosophila tissue polarity gene. *Genetics* 1990;**126**:401−16.
19. Krasnow RE, Wong LL, Adler PN. Dishevelled is a component of the frizzled signaling pathway in Drosophila. *Development* 1995;**121**: 4095−102.
20. Bhanot P, Brink M, Samos CH, Hsieh JC, Wang Y, Macke JP, et al. A new member of the frizzled family from Drosophila functions as a Wingless receptor. *Nature* 1996;**382**:225−30.
21. Dann CE, Hsieh JC, Rattner A, Sharma D, Nathans J, Leahy DJ. Insights into Wnt binding and signalling from the structures of two Frizzled cysteine-rich domains. *Nature* 2001;**412**:86−90.
22. Janda CY, Waghray D, Levin AM, Thomas C, Garcia KC. Structural basis of Wnt recognition by Frizzled. *Science* 2012;**337**:59−64.
23. Yang L, Yang Z, Li D, Liu Z, Zou Q, Yuan Y, et al. Overexpression of FZD1 and CAIX are associated with invasion, metastasis, and poor-prognosis of the pancreatic ductal adenocarcinoma. *Pathol Oncol Res* 2018;**24**:899−906.
24. Wright SC, Kozielewicz P, Kowalski-Jahn M, Petersen J, Bowin CF, Slodkowicz G, et al. A conserved molecular switch in class F receptors regulates receptor activation and pathway selection. *Nat Commun* 2019;**10**:667.
25. Schulte G, Scharf MM, Bous J, Voss JH, Grätz L, Kozielewicz P. Frizzleds act as dynamic pharmacological entities. *Trends Pharmacol Sci* 2024;**45**:419−29.
26. Tanaka S, Akiyoshi T, Mori M, Wands JR, Sugimachi K. A novel frizzled gene identified in human esophageal carcinoma mediates APC/beta-catenin signals. *Proc Natl Acad Sci USA* 1998;**95**: 10164−9.
27. Nagayama S, Fukukawa C, Katagiri T, Okamoto T, Aoyama T, Oyaizu N, et al. Therapeutic potential of antibodies against FZD 10, a cell-surface protein, for synovial sarcomas. *Oncogene* 2005;**24**: 6201−12.
28. Davis SL, Cardin DB, Shahda S, Lenz HJ, Dotan E, O'Neil BH, et al. A phase 1b dose escalation study of Wnt pathway inhibitor vantictumab in combination with nab-paclitaxel and gemcitabine in patients with previously untreated metastatic pancreatic cancer. *Invest N Drugs* 2020;**38**:821−30.
29. Chuan J, Li W, Pan S, Jiang Z, Shi J, Yang Z. Progress in the development of modulators targeting Frizzleds. *Pharmacol Res* 2024; **206**:107286.
30. Scharf MM, Kinsolving J, Grätz L, Voss JH, Carrasco-Busturia D, Forsberg B, et al. *In silico* docking yields small molecule negative allosteric modulators targeting the core of Frizzled 7. *Nat Commun* 2025;**16**:11138.
31. Kozielewicz P, Turku A, Bowin CF, Petersen J, Valnohova J, Cañizal MCA, et al. Structural insight into small molecule action on Frizzleds. *Nat Commun* 2020;**11**:414.
32. Generoso SF, Giustiniano M, La Regina G, Bottone S, Passacantilli S, Di Maro S, et al. Pharmacological folding chaperones act as allosteric ligands of Frizzled4. *Nat Chem Biol* 2015;**11**:280−6.
33. Nile AH, de Sousa EMF, Mukund S, Piskol R, Hansen S, Zhou L, et al. A selective peptide inhibitor of Frizzled 7 receptors disrupts intestinal stem cells. *Nat Chem Biol* 2018;**14**:582−90.
34. Riccio G, Bottone S, La Regina G, Badolati N, Passacantilli S, Rossi GB, et al. A negative allosteric modulator of WNT receptor frizzled 4 switches into an allosteric agonist. *Biochemistry* 2018;**57**: 839−51.
35. Zhao Y, Ren J, Hillier J, Lu W, Jones EY. Antiepileptic drug carbamazepine binds to a novel pocket on the Wnt receptor Frizzled-8. *J Med Chem* 2020;**63**:3252−60.
36. Logan CY, Nusse R. The Wnt signaling pathway in development and disease. *Annu Rev Cell Dev Biol* 2004;**20**:781−810.
37. Galluzzi L, Spranger S, Fuchs E, López-Soto A. WNT signaling in cancer immunosurveillance. *Trends Cell Biol* 2019;**29**:44−65.
38. Anastas JN, Moon RT. WNT signalling pathways as therapeutic targets in cancer. *Nat Rev Cancer* 2013;**13**:11−26.
39. Liu C, Li Y, Semenov M, Han C, Baeg GH, Tan Y, et al. Control of beta-catenin phosphorylation/degradation by a dual-kinase mechanism. *Cell* 2002;**108**:837−47.
40. Clevers H, Nusse R. Wnt/$\beta$-catenin signaling and disease. *Cell* 2012; **149**:1192−205.
41. Onyido EK, Sweeney E, Nateri AS. Wnt-signalling pathways and microRNAs network in carcinogenesis: experimental and bioinformatics approaches. *Mol Cancer* 2016;**15**:56.
42. Yu G, Chen Y, Hu Y, Zhou Y, Ding X, Zhou X. Roles of transducin-like enhancer of split (TLE) family proteins in tumorigenesis and immune regulation. *Front Cell Dev Biol* 2022;**10**:1010639.
43. Städeli R, Hoffmans R, Basler K. Transcription under the control of nuclear Arm/beta-catenin. *Curr Biol* 2006;**16**:R378−85.
44. Wolf J, Palmby TR, Gavard J, Williams BO, Gutkind JS. Multiple PPPS/TP motifs act in a combinatorial fashion to transduce Wnt signaling through LRP6. *FEBS Lett* 2008;**582**:255−61.
45. Stamos JL, Chu ML, Enos MD, Shah N, Weis WI. Structural basis of GSK-3 inhibition by N-terminal phosphorylation and by the Wnt receptor LRP6. *eLife* 2014;**3**:e01998.
46. Nusse R. Wnt signaling. *Cold Spring Harbor Perspect Biol* 2012;**4**: a011163.
47. Angers S, Moon RT. Proximal events in Wnt signal transduction. *Nat Rev Mol Cell Biol* 2009;**10**:468−77.
48. Liu J, Xiao Q, Xiao J, Niu C, Li Y, Zhang X, et al. Wnt/$\beta$-catenin signalling: function, biological mechanisms, and therapeutic opportunities. *Signal Transduct Targeted Ther* 2022;**7**:3.
49. Slusarski DC, Corces VG, Moon RT. Interaction of Wnt and a Frizzled homologue triggers G-protein-linked phosphatidylinositol signalling. *Nature* 1997;**390**:410−3.
50. Niehrs C. The complex world of WNT receptor signalling. *Nat Rev Mol Cell Biol* 2012;**13**:767−79.
51. Rogers S, Zhang C, Anagnostidis V, Liddle C, Fishel ML, Gielen F, et al. Cancer-associated fibroblasts influence Wnt/PCP signaling in gastric cancer cells by cytoneme-based dissemination of ROR2. *Proc Natl Acad Sci U S A* 2023;**120**:e2217612120.
52. Qin K, Yu M, Fan J, Wang H, Zhao P, Zhao G, et al. Canonical and noncanonical Wnt signaling: multilayered mediators, signaling mechanisms and major signaling crosstalk. *Genes Dis* 2024;**11**:103−34.
53. Daulat AM, Borg JP. Wnt/planar cell polarity signaling: new opportunities for cancer treatment. *Trends Cancer* 2017;**3**:113−25.
54. Gao Y, Chen N, Fu Z, Zhang Q. Progress of Wnt signaling pathway in osteoporosis. *Biomolecules* 2023;**13**:483.
55. McQuate A, Latorre-Esteves E, Barria A. A Wnt/calcium signaling cascade regulates neuronal excitability and trafficking of NMDARs. *Cell Rep* 2017;**21**:60−9.
56. Larasati Y, Boudou C, Koval A, Katanaev VL. Unlocking the Wnt pathway: therapeutic potential of selective targeting FZD(7) in cancer. *Drug Discov Today* 2022;**27**:777−92.
57. Dang S, Zhou J, Chen Y, Chen P, Ji M, Shi B, et al. Dynamic expression of ZNF382 and its tumor-suppressor role in hepatitis B virus-related hepatocellular carcinogenesis. *Oncogene* 2019;**38**: 4804−19.
58. Liu Y, Deng H, Liang L, Zhang G, Xia J, Ding K, et al. Depletion of VPS35 attenuates metastasis of hepatocellular carcinoma by restraining the Wnt/PCP signaling pathway. *Genes Dis* 2021;**8**:232−40.
59. Gujral TS, Chan M, Peshkin L, Sorger PK, Kirschner MW, MacBeath G. A noncanonical Frizzled2 pathway regulates epithelial−mesenchymal transition and metastasis. *Cell* 2014;**159**:844−56.
60. Golkowski M, Lau HT, Chan M, Kenerson H, Vidadala VN, Shoemaker A, et al. Pharmacoproteomics identifies kinase pathways that drive the epithelial−mesenchymal transition and drug resistance in hepatocellular carcinoma. *Cell Syst* 2020;**11**:196−207.e7.

61. Meng Z, Liu Q, Liu Y, Yang Y, Shao C, Zhang S. Frizzled-3 suppression overcomes multidrug chemoresistance by Wnt/$\beta$-catenin signaling pathway inhibition in hepatocellular carcinoma cells. *J Chemother* 2023;**35**:653−61.
62. Zhu GQ, Wang Y, Wang B, Liu WR, Dong SS, Chen EB, et al. Targeting HNRNPM inhibits cancer stemness and enhances anti-tumor immunity in Wnt-activated hepatocellular carcinoma. *Cell Mol Gastroenterol Hepatol* 2022;**13**:1413−47.
63. Li X, Lv J, Hou L, Guo X. Circ_0001955 acts as a miR-646 sponge to promote the proliferation, metastasis and angiogenesis of hepatocellular carcinoma. *Dig Dis Sci* 2022;**67**:2257−68.
64. Chen SZ, Ling Y, Yu LX, Song YT, Chen XF, Cao QQ, et al. 4-phenylbutyric acid promotes hepatocellular carcinoma *via* initiating cancer stem cells through activation of PPAR-$\alpha$. *Clin Transl Med* 2021;**11**:e379.
65. Krützfeldt J, Rösch N, Hausser J, Manoharan M, Zavolan M, Stoffel M. MicroRNA-194 is a target of transcription factor 1 (Tcf1, HNF1$\alpha$) in adult liver and controls expression of frizzled-6. *Hepatology* 2012;**55**:98−107.
66. Lopez A, Paturel A, Fares N, Pez F, Wang G, Gifu P, et al. Frizzled 7 drives amplification of cancer stem-cell subpopulations and the aggressiveness and poor differentiation of human hepatocellular carcinoma. *PLoS One* 2025;**20**:e0332768.
67. Gu Y, Wang Z, Liang G, Peng J, Zhang X, Yu T, et al. SIRT7 stabilizes $\beta$-catenin and promotes canonical Wnt activation *via* upregulating FZD7. *Life Sci* 2024;**359**:123240.
68. Chen Z, Huang C, Ma T, Jiang L, Tang L, Shi T, et al. Reversal effect of quercetin on multidrug resistance *via* FZD7/$\beta$-catenin pathway in hepatocellular carcinoma cells. *Phytomedicine* 2018;**43**:37−45.
69. Dai B, Ma Y, Yang T, Fan M, Yu R, Su Q, et al. Synergistic effect of berberine and HMQ1611 impairs cell proliferation and migration by regulating Wnt signaling pathway in hepatocellular carcinoma. *Phytother Res* 2019;**33**:745−55.
70. Fujimoto T, Tomizawa M, Yokosuka O. SiRNA of frizzled-9 suppresses proliferation and motility of hepatoma cells. *Int J Oncol* 2009;**35**:861−6.
71. Wang J, Yu H, Dong W, Zhang C, Hu M, Ma W, et al. *N*6-methyladenosine-mediated up-regulation of FZD10 regulates liver cancer stem cells' properties and lenvatinib resistance through WNT/$\beta$-catenin and Hippo signaling pathways. *Gastroenterology* 2023;**164**:990−1005.
72. Sun Q, Wang R, Luo J, Wang P, Xiong S, Liu M, et al. Notch1 promotes hepatitis B virus X protein-induced hepatocarcinogenesis *via* Wnt/$\beta$-catenin pathway. *Int J Oncol* 2014;**45**:1638−48.
73. Su W, Mo Y, Wu F, Guo K, Li J, Luo Y, et al. miR-135b reverses chemoresistance of non-small cell lung cancer cells by down-regulation of FZD1. *Biomed Pharmacother* 2016;**84**:123−9.
74. Hyun SY, Min HY, Lee HJ, Cho J, Boo HJ, Noh M, et al. Ninjurin1 drives lung tumor formation and progression by potentiating Wnt/$\beta$-Catenin signaling through Frizzled2-LRP6 assembly. *J Exp Clin Cancer Res* 2022;**41**:133.
75. Zhao H, Wu G, Luo Y, Xie Y, Han Y, Zhang D, et al. WNT5B promotes the malignant phenotype of non-small cell lung cancer *via* the FZD3−DVL3−RAC1−PCP−JNK pathway. *Cell Signal* 2024; **122**:111330.
76. Ji T, Li X, Li J, Wang G. *N*-glycosylation modification of Fzd4 is essential for the Fzd4-Wnt-$\beta$-catenin signalling axis. *J Cell Mol Med* 2025;**29**:e70539.
77. Chen D, Chen H, Zeng Y, Shi Y, Guo F, Fan J, et al. ZNF831-YTHDF1-DNMT1/3a feedback loop regulates lung carcinogenesis and progression through WNT7B-FZD5-$\beta$-catenin signalling axis. *Free Radic Biol Med* 2025;**241**:338−52.
78. Li K, Mao S, Li X, Zhao H, Wang J, Wang C, et al. Frizzled-7-targeting antibody (SHH002-hu1) potently suppresses non-small-cell lung cancer *via* Wnt/$\beta$-catenin signaling. *Cancer Sci* 2023;**114**: 2109−22.
79. Fu X, Li H, Liu C, Hu B, Li T, Wang Y. Long noncoding RNA AK126698 inhibits proliferation and migration of non-small cell lung cancer cells by targeting Frizzled-8 and suppressing Wnt/$\beta$-catenin signaling pathway. *OncoTargets Ther* 2016;**9**:3815−27.
80. Tennis MA, Van Scoyk M, Heasley LE, Vandervest K, Weiser-Evans M, Freeman S, et al. Prostacyclin inhibits non-small cell lung cancer growth by a frizzled 9-dependent pathway that is blocked by secreted frizzled-related protein 1. *Neoplasia* 2010;**12**:244−53.
81. Wu X, Zhan R, Cheng D, Chen L, Wang T, Tang X. Exosomal FZD10 derived from non-small cell lung cancer cells promotes angiogenesis of human umbilical venous endothelial cells *in vitro*. *Nan Fang Yi Ke Da Xue Xue Bao* 2022;**42**:1351−8.
82. Tong Y, Semba T, Nishimura A, Yonemura A, Yamazaki M, Wang H, et al. Frizzled-1 amplification promotes fibrosis in the gastric tumor microenvironment through the activation of fibroblasts *via* the SLIT2/ROBO1 axis. *Gastric Cancer* 2026;**29**:323−37.
83. Astudillo P. A non-canonical Wnt signature correlates with lower survival in gastric cancer. *Front Cell Dev Biol* 2021;**9**:633675.
84. Zhou S, Li D, Quan C, Yu Z, Feng Y, Wang S, et al. Pan-cancer profiling of FZD2 as a prognostic biomarker: integrative multi-omics analysis with experimental validation and functional characterization in gastric cancer. *Front Pharmacol* 2025;**16**:1534974.
85. Dong D, Na L, Zhou K, Wang Z, Sun Y, Zheng Q, et al. FZD5 prevents epithelial−mesenchymal transition in gastric cancer. *Cell Commun Signal* 2021;**19**:21.
86. Yan J, Liu T, Zhou X, Dang Y, Yin C, Zhang G. FZD6, targeted by miR-21, represses gastric cancer cell proliferation and migration *via* activating non-canonical wnt pathway. *Am J Transl Res* 2016;**8**:2354−64.
87. Guo S, Deng J, Wang P, Kou F, Wu Z, Zhang N, et al. The malignancy suppression and ferroptosis facilitation of BCL6 in gastric cancer mediated by FZD7 repression are strengthened by RNF180/RhoC pathway. *Cell Biosci* 2023;**13**:73.
88. Pi J, Wang W, Ji M, Wang X, Wei X, Jin J, et al. YTHDF1 promotes gastric carcinogenesis by controlling translation of FZD7. *Cancer Res* 2021;**81**:2651−65.
89. Tan XY, Li YT, Li HH, Ma LX, Zeng CM, Zhang TT, et al. WNT2-SOX4 positive feedback loop promotes chemoresistance and tumorigenesis by inducing stem-cell like properties in gastric cancer. *Oncogene* 2023;**42**:3062−74.
90. Chu CW, Ko HJ, Chou CH, Cheng TS, Cheng HW, Liang YH, et al. Thioridazine enhances P62-mediated autophagy and apoptosis through Wnt/$\beta$-catenin signaling pathway in glioma cells. *Int J Mol Sci* 2019;**20**:473.
91. Ran Y, Han S, Gao D, Chen X, Liu C. Interference of FZD2 suppresses proliferation, vasculogenic mimicry and stemness in glioma cells *via* blocking the Notch/NF-$\kappa$B signaling pathway. *Exp Ther Med* 2024;**28**:373.
92. Licón-Muñoz Y, Avalos V, Subramanian S, Granger B, Martinez F, García-Montaño LA, et al. Single-nucleus and spatial landscape of the sub-ventricular zone in human glioblastoma. *Cell Rep* 2025;**44**:115149.
93. El-Sehemy A, Selvadurai H, Ortin-Martinez A, Pokrajac N, Mamatjan Y, Tachibana N, et al. Norrin mediates tumor-promoting and -suppressive effects in glioblastoma *via* Notch and Wnt. *J Clin Investig* 2020;**130**:3069−86.
94. Jin X, Jeon H-Y, Joo KM, Kim J-K, Jin J, Kim SH, et al. Frizzled 4 regulates stemness and invasiveness of migrating glioma cells established by serial intracranial transplantation. *Cancer Res* 2011; **71**:3066−75.
95. Luo X, Zhong X, Zeng T, Li X, Yang T, Yue Q, et al. Isovalerylspiramycin I reprograms the immunosuppressive and temozolomide-resistant microenvironment by inhibiting the Frizzled-5/Wnt/β-catenin pathway in glioblastoma. *Research* 2025;**8**:828. Wash D C.
96. Chen Y, Cheng P, Huang W, Jing Y, Su J, Wu Z, et al. Association of Hsa_circ_0059511 with the sensitivity of the temozolomide chemotherapeutic treatment in human glioma cells. *Sci Rep* 2025;**15**:27761.
97. Huang T, Alvarez AA, Pangeni RP, Horbinski CM, Lu S, Kim SH, et al. A regulatory circuit of miR-125b/miR-20b and Wnt signalling controls glioblastoma phenotypes through FZD6-modulated pathways. *Nat Commun* 2016;**7**:12885.

98. Liu Q, Guan Y, Li Z, Wang Y, Liu Y, Cui R, et al. miR-504 suppresses mesenchymal phenotype of glioblastoma by directly targeting the FZD7-mediated Wnt-$\beta$-catenin pathway. *J Exp Clin Cancer Res* 2019;**38**:358.
99. Dreyer CA, VanderVorst K, Natwick D, Bell G, Sood P, Hernandez M, et al. A complex of Wnt/planar cell polarity signaling components Vangl1 and Fzd7 drives glioblastoma multiforme malignant properties. *Cancer Lett* 2023;**567**:216280.
100. Zhang Z, Schittenhelm J, Guo K, Bühring HJ, Trautmann K, Meyermann R, et al. Upregulation of frizzled 9 in astrocytomas. *Neuropathol Appl Neurobiol* 2006;**32**:615−24.
101. Tompa M, Kajtar B, Galik B, Gyenesei A, Kalman B. DNA methylation and protein expression of Wnt pathway markers in progressive glioblastoma. *Pathol Res Pract* 2021;**222**:153429.
102. Cai MY, Yin P, Wang ZW, Huang YZ, Wang YX, Wu KF, et al. Dual regulation of FZD1/7 by IGF2BP3 enhances stem-like properties and carboplatin resistance in triple-negative breast cancer. *Cancer Lett* 2025;**632**:217944.
103. Tuluhong D, Chen T, Wang J, Zeng H, Li H, Dunzhu W, et al. FZD2 promotes TGF-$\beta$-induced epithelial-to-mesenchymal transition in breast cancer *via* activating notch signaling pathway. *Cancer Cell Int* 2021;**21**:199.
104. Mo D, Jiang P, Yang Y, Mao X, Tan X, Tang X, et al. A tRNA fragment, 5′-tiRNAVal, suppresses the Wnt/$\beta$-catenin signaling pathway by targeting FZD3 in breast cancer. *Cancer Lett* 2019;**457**: 60−73.
105. Sun Y, Wang Z, Na L, Dong D, Wang W, Zhao C. FZD5 contributes to TNBC proliferation, DNA damage repair and stemness. *Cell Death Dis* 2020;**11**:1060.
106. Wan X, Guan S, Hou Y, Qin Y, Zeng H, Yang L, et al. FOSL2 promotes VEGF-independent angiogenesis by transcriptionnally activating Wnt5a in breast cancer-associated fibroblasts. *Theranostics* 2021;**11**:4975−91.
107. Corda G, Sala G, Lattanzio R, Iezzi M, Sallese M, Fragassi G, et al. Functional and prognostic significance of the genomic amplification of frizzled 6 (FZD6) in breast cancer. *J Pathol* 2017;**241**:350−61.
108. Hoover EC, Day ES. Antibody/siRNA nanocarriers against Wnt signaling suppress oncogenic and stem-like behavior in triple-negative breast cancer cells. *J Biomed Mater Res* 2025;**113**:e37867.
109. Wang C, Wu L, Li X, Mao S, Wang Z, Xie H, et al. Frizzled-7-targeting antibody-derived bifunctional protein retargets NK cells against triple-negative breast cancer cells *via* MICA-NKG2D axis. *J Immunother Cancer* 2025;**13**:e009621.
110. Hoover EC, Ruggiero OM, Swingler RN, Day ES. FZD7-targeted nanoparticles to enhance doxorubicin treatment of triple-negative breast cancer. *ACS Omega* 2024;**9**:14323−35.
111. Al-Zahrani MH, Assidi M, Pushparaj PN, Al-Maghrabi J, Zari A, Abusanad A, et al. Expression pattern, prognostic value and potential microRNA silencing of FZD8 in breast cancer. *Oncol Lett* 2023;**26**: 477.
112. Yang L, Wu X, Wang Y, Zhang K, Wu J, Yuan YC, et al. FZD7 has a critical role in cell proliferation in triple negative breast cancer. *Oncogene* 2011;**30**:4437−46.
113. Gong C, Qu S, Lv XB, Liu B, Tan W, Nie Y, et al. BRMS1L suppresses breast cancer metastasis by inducing epigenetic silence of FZD10. *Nat Commun* 2014;**5**:5406.
114. Liu H, Chen Y, Zhou F, Jie L, Pu L, Ju J, et al. Sox9 regulates hyperexpression of Wnt1 and Fzd1 in human osteosarcoma tissues and cells. *Int J Clin Exp Pathol* 2014;**7**:4795−805.
115. Yu B, Liu L, Cai F, Peng Y, Tang X, Zeng D, et al. The synergistic anticancer effect of the bromodomain inhibitor OTX015 and histone deacetylase 6 inhibitor WT-161 in osteosarcoma. *Cancer Cell Int* 2022;**22**:64.
116. Zhu S, Liu Y, Wang X, Wang J, Xi G. lncRNA SNHG10 promotes the proliferation and invasion of osteosarcoma *via* Wnt/$\beta$-catenin signaling. *Mol Ther Nucleic Acids* 2020;**22**:957−70.
117. Feng ZH, Zheng L, Yao T, Tao SY, Wei XA, Zheng ZY, et al. EIF4A3-induced circular RNA PRKAR1B promotes osteosarcoma progression by miR-361-3p-mediated induction of FZD4 expression. *Cell Death Dis* 2021;**12**:1025.
118. Daino K, Ugolin N, Altmeyer-Morel S, Guilly MN, Chevillard S. Gene expression profiling of alpha-radiation-induced rat osteosarcomas: identification of dysregulated genes involved in radiation-induced tumorigenesis of bone. *Int J Cancer* 2009;**125**:612−20.
119. Xie C, Chen B, Wu B, Guo J, Shi Y, Cao Y. CircSAMD4A regulates cell progression and epithelial−mesenchymal transition by sponging miR-342-3p *via* the regulation of FZD7 expression in osteosarcoma. *Int J Mol Med* 2020;**46**:107−18.
120. Wang Q, Liu H, Wang Q, Zhou F, Liu Y, Zhang Y, et al. Involvement of c-Fos in cell proliferation, migration, and invasion in osteosarcoma cells accompanied by altered expression of Wnt2 and Fzd9. *PLoS One* 2017;**12**:e0180558.
121. Zhao SJ, Jiang YQ, Xu NW, Li Q, Zhang Q, Wang SY, et al. SPARCL1 suppresses osteosarcoma metastasis and recruits macrophages by activation of canonical WNT/$\beta$-catenin signaling through stabilization of the WNT-receptor complex. *Oncogene* 2018;**37**: 1049−61.
122. Alawyia B, Constantinou C. Hepatocellular carcinoma: a narrative review on current knowledge and future prospects. *Curr Treat Options Oncol* 2023;**24**:711−24.
123. Bengochea A, de Souza MM, Lefrançois L, Le Roux E, Galy O, Chemin I, et al. Common dysregulation of Wnt/Frizzled receptor elements in human hepatocellular carcinoma. *Br J Cancer* 2008;**99**: 143−50.
124. Ma K, Wu H, Ji L. Construction of HBV gene-related prognostic and diagnostic models for hepatocellular carcinoma. *Front Genet* 2022; **13**:1065644.
125. Chan KK, Lo RC. Deregulation of Frizzled receptors in hepatocellular carcinoma. *Int J Mol Sci* 2018;**19**:313.
126. Song J, Gao L, Yang G, Tang S, Xie H, Wang Y, et al. MiR-199a regulates cell proliferation and survival by targeting FZD7. *PLoS One* 2014;**9**:e110074.
127. Xue Y, Chen C, Xu W, Xu H, Zheng J, Gu Y. Downregulation of Frizzled-7 induces the apoptosis of hepatocellular carcinoma cells through inhibition of NF-$\kappa$B. *Oncol Lett* 2018;**15**:7693−701.
128. Katoh M. Multi-layered prevention and treatment of chronic inflammation, organ fibrosis and cancer associated with canonical WNT/$\beta$-catenin signaling activation (Review). *Int J Mol Med* 2018; **42**:713−25.
129. Dehan E, Ben-Dor A, Liao W, Lipson D, Frimer H, Rienstein S, et al. Chromosomal aberrations and gene expression profiles in non-small cell lung cancer. *Lung Cancer* 2007;**56**:175−84.
130. Sompel K, Dwyer-Nield LD, Smith AJ, Elango AP, Vanderlinden LA, Kopf K, et al. Loss of Frizzled 9 in lung cells alters epithelial phenotype and promotes premalignant lesion development. *Front Oncol* 2022;**12**:815737.
131. Sompel K, Dwyer-Nield LD, Smith AJ, Elango A, Backos DS, Zhang B, et al. Iloprost requires the Frizzled-9 receptor to prevent lung cancer. *iScience* 2022;**25**:104442.
132. Avasarala S, Bikkavilli RK, Van Scoyk M, Zhang W, Lapite A, Hostetter L, et al. Heterotrimeric G-protein, G$\alpha$16, is a critical downstream effector of non-canonical Wnt signaling and a potent inhibitor of transformed cell growth in non small cell lung cancer. *PLoS One* 2013;**8**:e76895.
133. Sundar R, Nakayama I, Markar SR, Shitara K, van Laarhoven HWM, Janjigian YY, et al. Gastric cancer. *Lancet* 2025;**405**:2087−102.
134. Kirikoshi H, Sekihara H, Katoh M. Expression profiles of 10 members of Frizzled gene family in human gastric cancer. *Int J Oncol* 2001;**19**:767−71.
135. Flanagan DJ, Barker N, Costanzo NSD, Mason EA, Gurney A, Meniel VS, et al. Frizzled-7 is required for Wnt signaling in gastric tumors with and without APC mutations. *Cancer Res* 2019;**79**:970−81.
136. Fujiya K, Ohshima K, Kitagawa Y, Hatakeyama K, Nagashima T, Aizawa D, et al. Aberrant expression of Wnt/$\beta$-catenin signaling pathway genes in aggressive malignant gastric gastrointestinal stromal tumors. *Eur J Surg Oncol* 2020;**46**:1080−7.

137. Sun M, Tan Z, Lin K, Chang Z, Yang Z, Yang X, et al. FPR3 sustains the immunosuppression of tumor-associated macrophages and accelerates the progression of gastric adenocarcinoma. *Oncogene* 2025; **44**:4309−23.
138. Chen J, Jiang F, Niu K, Zhao H, Li LI, Yu H. A novel Wnt/$\beta$-catenin signaling gene signature for progression and metastasis of gastric cancer. *Oncol Res* 2025;**33**:1199−215.
139. Koushyar S, Powell AG, Vincan E, Phesse TJ. Targeting Wnt signaling for the treatment of gastric cancer. *Int J Mol Sci* 2020;**21**: 3927.
140. Lee Y, Lee JK, Ahn SH, Lee J, Nam DH. WNT signaling in glioblastoma and therapeutic opportunities. *Lab Invest* 2016;**96**:137−50.
141. Phon BWS, Bhuvanendran S, Ayub Q, Radhakrishnan AK, Kamarudin MNA. Identification of prominent genes between 3D glioblastoma models and clinical samples *via* GEO/TCGA/CGGA data analysis. *Biology (Basel)* 2023;**12**:648.
142. Hirano H, Yonezawa H, Yunoue S, Habu M, Uchida H, Yoshioka T, et al. Immunoreactivity of Wnt5a, Fzd2, Fzd6, and Ryk in glioblastoma: evaluative methodology for DAB chromogenic immunostaining. *Brain Tumor Pathol* 2014;**31**:85−93.
143. Sun X, Jabeen A, Zhang L, Li C, Serfraz S. G-protein-coupled receptor FZD7 as a therapeutic target in glioblastoma: multi-cohort validation and identification of cycloartobiloxanthone as an inhibitor. *Bioorg Chem* 2025;**162**:108616.
144. Kim J, Harper A, McCormack V, Sung H, Houssami N, Morgan E, et al. Global patterns and trends in breast cancer incidence and mortality across 185 countries. *Nat Med* 2025;**31**:1154−62.
145. Yin P, Wang W, Zhang Z, Bai Y, Gao J, Zhao C. Wnt signaling in human and mouse breast cancer: focusing on Wnt ligands, receptors and antagonists. *Cancer Sci* 2018;**109**:3368−75.
146. Wu CCN, De Luna N, Hairston E, Jeffs ED, Key A, Adams SR, et al. FZD7 expression marks mammary tumor-initiating cells. *Proc Natl Acad Sci U S A* 2025;**122**:e2522465122.
147. Yin P, Bai Y, Wang Z, Sun Y, Gao J, Na L, et al. Non-canonical Fzd7 signaling contributes to breast cancer mesenchymal-like stemness involving Col6a1. *Cell Commun Signal* 2020;**18**:143.
148. Yin P, Wang W, Gao J, Bai Y, Wang Z, Na L, et al. Fzd2 contributes to breast cancer cell mesenchymal-like stemness and drug resistance. *Oncol Res* 2020;**28**:273−84.
149. Wang H, Zhu T, Yang K, Xu C, Zhang Z, Liu G, et al. Decoding the immune microenvironment in osteosarcoma: new insights into checkpoints, vaccines, and CAR-T cells. *Front Oncol* 2025;**15**: 1702219.
150. Dijksterhuis JP, Petersen J, Schulte G. WNT/Frizzled signalling: receptor−ligand selectivity with focus on FZD-G protein signalling and its physiological relevance: IUPHAR Review 3. *Br J Pharmacol* 2014;**171**:1195−209.
151. Umar SA, Dong B, Nihal M, Chang H. Frizzled receptors in melanomagenesis: from molecular interactions to target identification. *Front Oncol* 2022;**12**:1096134.
152. Bats ML, Peghaire C, Delobel V, Dufourcq P, Couffinhal T, Duplàa C. Wnt/frizzled signaling in endothelium: a major player in blood-retinal- and blood−brain-barrier integrity. *Cold Spring Harb Perspect Med* 2022;**12**:a041219.
153. MacDonald BT, He X. Frizzled and LRP5/6 receptors for Wnt/$\beta$-catenin signaling. *Cold Spring Harbor Perspect Biol* 2012;**4**: a007880.
154. Ding J, Lee SJ, Vlahos L, Yuki K, Rada CC, van Unen V, et al. Therapeutic blood-brain barrier modulation and stroke treatment by a bioengineered FZD(4)-selective WNT surrogate in mice. *Nat Commun* 2023;**14**:2947.
155. Chidiac R, Abedin M, Macleod G, Yang A, Thibeault PE, Blazer LL, et al. A Norrin/Wnt surrogate antibody stimulates endothelial cell barrier function and rescues retinopathy. *EMBO Mol Med* 2021;**13**: e13977.
156. Ke J, Harikumar KG, Erice C, Chen C, Gu X, Wang L, et al. Structure and function of Norrin in assembly and activation of a Frizzled 4-Lrp5/6 complex. *Genes Dev* 2013;**27**:2305−19.
157. Chang TH, Hsieh FL, Zebisch M, Harlos K, Elegheert J, Jones EY. Structure and functional properties of Norrin mimic Wnt for signalling with Frizzled4, Lrp5/6, and proteoglycan. *eLife* 2015;**4**:e06554.
158. Shen G, Ke J, Wang Z, Cheng Z, Gu X, Wei Y, et al. Structural basis of the Norrin-Frizzled 4 interaction. *Cell Res* 2015;**25**:1078−81.
159. Zhang M, Chen T, Lu X, Lan X, Chen Z, Lu S. G protein-coupled receptors (GPCRs): advances in structures, mechanisms, and drug discovery. *Signal Transduct Targeted Ther* 2024;**9**:88.
160. Yang S, Wu Y, Xu TH, de Waal PW, He Y, Pu M, et al. Crystal structure of the Frizzled 4 receptor in a ligand-free state. *Nature* 2018;**560**:666−70.
161. Martinez-Marin D, Stroman GC, Fulton CJ, Pruitt K. Frizzled receptors: gatekeepers of Wnt signaling in development and disease. *Front Cell Dev Biol* 2025;**13**:1599355.
162. Gammons MV, Renko M, Johnson CM, Rutherford TJ, Bienz M. Wnt signalosome assembly by DEP domain swapping of dishevelled. *Mol Cell* 2016;**64**:92−104.
163. Qian Y, Ma Z, Xu Z, Duan Y, Xiong Y, Xia R, et al. Structural basis of Frizzled 4 in recognition of dishevelled 2 unveils mechanism of WNT signaling activation. *Nat Commun* 2024;**15**:7644.
164. Xu L, Chen B, Schihada H, Wright SC, Turku A, Wu Y, et al. Cryo-EM structure of constitutively active human Frizzled 7 in complex with heterotrimeric G(s). *Cell Res* 2021;**31**:1311−4.
165. Yin Y, Sun Y, Yao H, Yu F, Jia Q, Hu C, et al. TMEM105 modulates disulfidptosis and tumor growth in pancreatic cancer *via* the $\beta$-catenin−c-MYC−GLUT1 axis. *Int J Biol Sci* 2025;**21**:1932−48.
166. Wang MT, Holderfield M, Galeas J, Delrosario R, To MD, Balmain A, et al. K-Ras promotes tumorigenicity through suppression of non-canonical Wnt signaling. *Cell* 2015;**163**:1237−51.
167. Lee HJ, Bao J, Miller A, Zhang C, Wu J, Baday YC, et al. Structure-based discovery of novel small molecule Wnt signaling inhibitors by targeting the cysteine-rich domain of Frizzled. *J Biol Chem* 2015; **290**:30596−606.
168. Alves Pinto I, Freitas Da Silveira NJ. *In silico* identification of potential inhibitors of the Wnt signaling pathway in human breast cancer. *J Comput Biol* 2020;**27**:999−1010.
169. Li N, Ge Q, Guo Q, Tao Y. Identification and functional validation of FZD8-specific antibodies. *Int J Biol Macromol* 2024;**254**:127846.
170. Pavlovic Z, Adams JJ, Blazer LL, Gakhal AK, Jarvik N, Steinhart Z, et al. A synthetic anti-Frizzled antibody engineered for broadened specificity exhibits enhanced anti-tumor properties. *mAbs* 2018;**10**: 1157−67.
171. Fukukawa C, Hanaoka H, Nagayama S, Tsunoda T, Toguchida J, Endo K, et al. Radioimmunotherapy of human synovial sarcoma using a monoclonal antibody against FZD10. *Cancer Sci* 2008;**99**:432−40.
172. Riley RS, Day ES. Frizzled7 antibody-functionalized nanoshells enable multivalent binding for Wnt signaling inhibition in triple negative breast cancer cells. *Small* 2017;**13**:1700544.
173. Steinhart Z, Pavlovic Z, Chandrashekhar M, Hart T, Wang X, Zhang X, et al. Genome-wide CRISPR screens reveal a Wnt-FZD5 signaling circuit as a druggable vulnerability of RNF43-mutant pancreatic tumors. *Nat Med* 2017;**23**:60−8.
174. Raman S, Beilschmidt M, To M, Lin K, Lui F, Jmeian Y, et al. Structure-guided design fine-tunes pharmacokinetics, tolerability, and antitumor profile of multispecific frizzled antibodies. *Proc Natl Acad Sci U S A* 2019;**116**:6812−7.
175. Zarei N, Fazeli M, Mohammadi M, Nejatollahi F. Cell growth inhibition and apoptosis in breast cancer cells induced by anti-FZD7 scFvs: involvement of bioinformatics-based design of novel epitopes. *Breast Cancer Res Treat* 2018;**169**:427−36.
176. Do M, Wu CCN, Sonavane PR, Juarez EF, Adams SR, Ross J, et al. A FZD7-specific antibody−drug conjugate induces ovarian tumor regression in preclinical models. *Mol Cancer Therapeut* 2022;**21**: 113−24.
177. Sudo H, Tsuji AB, Sugyo A, Harada Y, Nagayama S, Katagiri T, et al. FZD10-targeted $\alpha$-radioimmunotherapy with (225) Ac-labeled OTSA101 achieves complete remission in a synovial sarcoma model. *Cancer Sci* 2022;**113**:721−32.

178. Guo S, Zhao Y, Yuan Y, Liao Y, Jiang X, Wang L, et al. Progress in the development of macrophage migration inhibitory factor small-molecule inhibitors. *Eur J Med Chem* 2025;**286**:117280.
179. Dai E, Liu M, Li S, Zhang X, Wang S, Zhao R, et al. Identification of novel FZD4 mutations in familial exudative vitreoretinopathy and investigating the pathogenic mechanisms of FZD4 mutations. *Investig Ophthalmol Vis Sci* 2024;**65**:1.
180. El Beaino M, Rassy E, Hadid B, Araujo DM, Pavlidis N, Lin PP. Synovial sarcoma: a complex disease with multifaceted signaling and epigenetic landscapes. *Curr Oncol Rep* 2020;**22**:124.
181. Dijksterhuis JP, Baljinnyam B, Stanger K, Sercan HO, Ji Y, Andres O, et al. Systematic mapping of WNT-FZD protein interactions reveals functional selectivity by distinct WNT-FZD pairs. *J Biol Chem* 2015;**290**:6789−98.
182. Zheng S, Sheng R. The emerging understanding of Frizzled receptors. *FEBS Lett* 2024;**598**:1939−54.
183. Schrage R, Kostenis E. Functional selectivity and dualsteric/bitopic GPCR targeting. *Curr Opin Pharmacol* 2017;**32**:85−90.
184. Hillier J, Zhao Y, Carrique L, Malinauskas T, Ruza RR, Chang TH, et al. Structural insights into Frizzled3 through nanobody modulators. *Nat Commun* 2024;**15**:7228.
185. Diamond JR, Becerra C, Richards D, Mita A, Osborne C, O'Shaughnessy J, et al. Phase Ib clinical trial of the anti-frizzled antibody vantictumab (OMP-18R5) plus paclitaxel in patients with locally advanced or metastatic HER2-negative breast cancer. *Breast Cancer Res Treat* 2020;**184**:53−62.
186. Albers J, Keller J, Baranowsky A, Beil FT, Catala-Lehnen P, Schulze J, et al. Canonical Wnt signaling inhibits osteoclastogenesis independent of osteoprotegerin. *J Cell Biol* 2013;**200**:537−49.
187. Yu S, Yerges-Armstrong LM, Chu Y, Zmuda JM, Zhang Y. AP2 suppresses osteoblast differentiation and mineralization through down-regulation of Frizzled-1. *Biochem J* 2015;**465**:395−404.
188. Zhu X, Xu M, Leu NA, Morrisey EE, Millar SE. FZD2 regulates limb development by mediating $\beta$-catenin-dependent and -independent Wnt signaling pathways. *Dis Model Mech* 2023;**16**. dmm049876.
189. Casadó-Anguera V, Casadó V. Unmasking allosteric-binding sites: novel targets for GPCR drug discovery. *Expet Opin Drug Discov* 2022;**17**:897−923.
190. Zhang M, Lan X, Li X, Lu S. Pharmacologically targeting intracellular allosteric sites of GPCRs for drug discovery. *Drug Discov Today* 2023;**28**:103803.
191. Bous J, Kinsolving J, Grätz L, Scharf MM, Voss JH, Selcuk B, et al. Structural basis of frizzled 7 activation and allosteric regulation. *Nat Commun* 2024;**15**:7422.
192. Yoshikawa AM, Rangel AE, Zheng L, Wan L, Hein LA, Hariri AA, et al. A massively parallel screening platform for converting aptamers into molecular switches. *Nat Commun* 2023;**14**:2336.
193. Turku A, Schihada H, Kozielewicz P, Bowin CF, Schulte G. Residue 6.43 defines receptor function in class F GPCRs. *Nat Commun* 2021;**12**:3919.
194. Liu F, Wu CG, Tu CL, Glenn I, Meyerowitz J, Kaplan AL, et al. Large library docking identifies positive allosteric modulators of the calcium-sensing receptor. *Science* 2024;**385**. eado1868.
195. Thal DM, Glukhova A, Sexton PM, Christopoulos A. Structural insights into G-protein-coupled receptor allostery. *Nature* 2018;**559**:45−53.
196. Chen G, Bláhová J, Staffen N, Hübner H, Nunhöfer N, Qiu C, et al. Mechanism and function of GPR3 regulated by a negative allosteric modulator. *Nat Commun* 2025;**16**:7988.
197. Myslivecek J. Multitargeting nature of muscarinic orthosteric agonists and antagonists. *Front Physiol* 2022;**13**:974160.
198. Park J, Zuo H, Frangaj A, Fu Z, Yen LY, Zhang Z, et al. Symmetric activation and modulation of the human calcium-sensing receptor. *Proc Natl Acad Sci U S A* 2021;**118**:e2115849118.
199. Shao Z, Yan W, Chapman K, Ramesh K, Ferrell AJ, Yin J, et al. Structure of an allosteric modulator bound to the CB1 cannabinoid receptor. *Nat Chem Biol* 2019;**15**:1199−205.
200. Liu H, Kim HR, Deepak R, Wang L, Chung KY, Fan H, et al. Orthosteric and allosteric action of the C5a receptor antagonists. *Nat Struct Mol Biol* 2018;**25**:472−81.
201. Liu X, Kaindl J, Korczynska M, Stößel A, Dengler D, Stanek M, et al. An allosteric modulator binds to a conformational hub in the $\beta(2)$ adrenergic receptor. *Nat Chem Biol* 2020;**16**:749−55.
202. Chen YN, LaMarche MJ, Chan HM, Fekkes P, Garcia-Fortanet J, Acker MG, et al. Allosteric inhibition of SHP2 phosphatase inhibits cancers driven by receptor tyrosine kinases. *Nature* 2016;**535**:148−52.
203. Du J, Wang D, Fan H, Xu C, Tai L, Lin S, et al. Structures of human mGlu2 and mGlu7 homo- and heterodimers. *Nature* 2021;**594**:589−93.
204. Nasrallah C, Cannone G, Briot J, Rottier K, Berizzi AE, Huang CY, et al. Agonists and allosteric modulators promote signaling from different metabotropic glutamate receptor 5 conformations. *Cell Rep* 2021;**36**:109648.
205. Oswald C, Rappas M, Kean J, Doré AS, Errey JC, Bennett K, et al. Intracellular allosteric antagonism of the CCR9 receptor. *Nature* 2016;**540**:462−5.
206. Conflitti P, Lyman E, Sansom MSP, Hildebrand PW, Gutiérrez-de-Terán H, Carloni P, et al. Functional dynamics of G protein-coupled receptors reveal new routes for drug discovery. *Nat Rev Drug Discov* 2025;**24**:251−75.
207. Persechino M, Hedderich JB, Kolb P, Hilger D. Allosteric modulation of GPCRs: from structural insights to *in silico* drug discovery. *Pharmacol Ther* 2022;**237**:108242.
208. Lu S, He X, Ni D, Zhang J. Allosteric modulator discovery: from serendipity to structure-based design. *J Med Chem* 2019;**62**:6405−21.
209. Davis MI, Hunt JP, Herrgard S, Ciceri P, Wodicka LM, Pallares G, et al. Comprehensive analysis of kinase inhibitor selectivity. *Nat Biotechnol* 2011;**29**:1046−51.
210. Wenthur CJ, Gentry PR, Mathews TP, Lindsley CW. Drugs for allosteric sites on receptors. *Annu Rev Pharmacol Toxicol* 2014;**54**:165−84.
211. Qiao H, Yuan Z, Xing L, He BX, Ma LY, He ZX. Innovative medicinal chemistry strategies for improving target binding kinetics in drug discovery. *J Med Chem* 2025;**68**:22116−44.
212. Slosky LM, Caron MG, Barak LS. Biased allosteric modulators: new frontiers in GPCR drug discovery. *Trends Pharmacol Sci* 2021;**42**:283−99.
213. Hartl FU, Bracher A, Hayer-Hartl M. Molecular chaperones in protein folding and proteostasis. *Nature* 2011;**475**:324−32.
214. Li R, He X, Wu C, Li M, Zhang J. Advances in structure-based allosteric drug design. *Curr Opin Struct Biol* 2025;**90**:102974.
215. Chen X, Wang K, Chen J, Wu C, Mao J, Song Y, et al. Integrative residue-intuitive machine learning and MD approach to unveil allosteric site and mechanism for $\beta$2AR. *Nat Commun* 2024;**15**:8130.
216. Huang J, Tang G, Liu N, Li X, Lu S. Recent advances in computational strategies for allosteric site prediction: machine learning, molecular dynamics, and network-based approaches. *Drug Discov Today* 2025;**30**:104466.
217. Maity D, Qiao B. AlloBench: a data set pipeline for the development and benchmarking of allosteric site prediction tools. *ACS Omega* 2025;**10**:17973−82.
218. He J, Liu X, Zhu C, Zha J, Li Q, Zhao M, et al. ASD2023: towards the integrating landscapes of allosteric knowledgebase. *Nucleic Acids Res* 2024;**52**. D376-d83.
219. Hu J, Szymczak S. A review on longitudinal data analysis with random forest. *Briefings Bioinf* 2023;**24**. bbad002.
220. Maltarollo VG, Kronenberger T, Espinoza GZ, Oliveira PR, Honorio KM. Advances with support vector machines for novel drug discovery. *Expet Opin Drug Discov* 2019;**14**:23−33.
221. Schindele A, Krebold A, Heiß U, Nimptsch K, Pfaehler E, Berr C, et al. Interpretable machine learning for thyroid cancer recurrence predicton: leveraging XGBoost and SHAP analysis. *Eur J Radiol* 2025;**186**:112049.

222. Huang W, Lu S, Huang Z, Liu X, Mou L, Luo Y, et al. Allosite: a method for predicting allosteric sites. *Bioinformatics* 2013;**29**:2357−9.
223. Wang Y, Boadu F, Cheng J. MPBind: a multitask protein binding site predictor using protein language models and equivariant GNNs. *Bioinformatics* 2025;**41**. btaf589.
224. Gamouh H, Novotný M, Hoksza D. Hybrid protein−ligand binding residue prediction with protein language models: does the structure matter?. *Bioinformatics* 2025;**41**. btaf431.
225. Ebeid IA, Tang H, Gu P. Inferred global dense residue transition graphs from primary structure sequences enable protein interaction prediction *via* directed graph convolutional neural networks. *Front Bioinform* 2025;**5**:1651623.
226. Zhu J, Wang J, Han W, Xu D. Neural relational inference to learn long-range allosteric interactions in proteins from molecular dynamics simulations. *Nat Commun* 2022;**13**:1661.
227. Lin Z, Akin H, Rao R, Hie B, Zhu Z, Lu W, et al. Evolutionary-scale prediction of atomic-level protein structure with a language model. *Science* 2023;**379**:1123−30.
228. Tian H, Xiao S, Jiang X, Tao P. PASSerRank: prediction of allosteric sites with learning to rank. *J Comput Chem* 2023;**44**:2223−9.
229. Song K, Liu X, Huang W, Lu S, Shen Q, Zhang L, et al. Improved method for the identification and validation of allosteric sites. *J Chem Inf Model* 2017;**57**:2358−63.
230. Shi Y. A glimpse of structural biology through X-ray crystallography. *Cell* 2014;**159**:995−1014.
231. Wang J, Wang Y, Cui WW, Huang Y, Yang Y, Liu Y, et al. Druggable negative allosteric site of P2X3 receptors. *Proc Natl Acad Sci U S A* 2018;**115**:4939−44.
232. Van Drie JH, Tong L. Cryo-EM as a powerful tool for drug discovery. *Bioorg Med Chem Lett* 2020;**30**:127524.
233. Zhu KF, Yuan C, Du YM, Sun KL, Zhang XK, Vogel H, et al. Applications and prospects of cryo-EM in drug discovery. *Milit Med Res* 2023;**10**:10.
234. Grutsch S, Brüschweiler S, Tollinger M. NMR methods to study dynamic allostery. *PLoS Comput Biol* 2016;**12**:e1004620.
235. Lisi GP, Loria JP. Solution NMR spectroscopy for the study of enzyme allostery. *Chem Rev* 2016;**116**:6323−69.
236. Miao Y, Goldfeld DA, Moo EV, Sexton PM, Christopoulos A, McCammon JA, et al. Accelerated structure-based design of chemically diverse allosteric modulators of a muscarinic G protein-coupled receptor. *Proc Natl Acad Sci U S A* 2016;**113**:E5675−84.
237. Abdul-Ridha A, López L, Keov P, Thal DM, Mistry SN, Sexton PM, et al. Molecular determinants of allosteric modulation at the M1 muscarinic acetylcholine receptor. *J Biol Chem* 2014;**289**:6067−79.
238. Wang X, Liu D, Shen L, Li F, Li Y, Yang L, et al. A genetically encoded F-19 NMR probe reveals the allosteric modulation mechanism of cannabinoid receptor 1. *J Am Chem Soc* 2021;**143**:16320−5.
239. Congreve M, Oswald C, Marshall FH. Applying structure-based drug design approaches to allosteric modulators of GPCRs. *Trends Pharmacol Sci* 2017;**38**:837−47.
240. van der Westhuizen ET, Valant C, Sexton PM, Christopoulos A. Endogenous allosteric modulators of G protein-coupled receptors. *J Pharmacol Exp Therapeut* 2015;**353**:246−60.
241. Hothersall JD, Guo D, Sarda S, Sheppard RJ, Chen H, Keur W, et al. Structure−activity relationships of the sustained effects of adenosine A2A receptor agonists driven by slow dissociation kinetics. *Mol Pharmacol* 2017;**91**:25−38.
242. Wu Y, Shi W, Li C, Liu X, Jiang Y, Qiu Y, et al. Managing strategies of chemotherapy and radiotherapy-induced oral mucositis. *Cancer Treat Rev* 2025;**133**:102883.
243. Peng Y, Yu M, Li B, Zhang S, Cheng J, Wu F, et al. Advances in nanocarrier-mediated cancer therapy: progress in immunotherapy, chemotherapy, and radiotherapy. *Chin Med J (Engl)* 2025;**138**:1927−44.
244. Khan MM, Yalamarty SSK, Rajmalani BA, Filipczak N, Torchilin VP. Recent strategies to overcome breast cancer resistance. *Crit Rev Oncol Hematol* 2024;**197**:104351.
245. Tang L, Huang Z, Mei H, Hu Y. Immunotherapy in hematologic malignancies: achievements, challenges and future prospects. *Signal Transduct Targeted Ther* 2023;**8**:306.
246. O'Donnell JS, Teng MWL, Smyth MJ. Cancer immunoediting and resistance to T cell-based immunotherapy. *Nat Rev Clin Oncol* 2019;**16**:151−67.
247. Wang B, Tian T, Kalland KH, Ke X, Qu Y. Targeting Wnt/$\beta$-catenin signaling for cancer immunotherapy. *Trends Pharmacol Sci* 2018;**39**:648−58.
248. Shah K, Panchal S, Patel B. Porcupine inhibitors: novel and emerging anti-cancer therapeutics targeting the Wnt signaling pathway. *Pharmacol Res* 2021;**167**:105532.
249. Mehta CC, Bhatt HG. Tankyrase inhibitors as antitumor agents: a patent update (2013−2020). *Expert Opin Ther Pat* 2021;**31**:645−61.
250. Hmila I, Katanaev VL. Therapeutic targeting of FZD receptor proteins with biologics in cancer. *Drug Discov Today* 2026;**31**:104621.
251. Miao Y, McCammon JA. G-protein coupled receptors: advances in simulation and drug discovery. *Curr Opin Struct Biol* 2016;**41**:83−9.